NASA Technical Memorandum 102155

# Orbital Debris Research at NASA Johnson Space Center, 1986 - 1988

Robert C. Reynolds, Ph.D., and
Andrew E. Potter, Jr., Ph.D.

September 1989



National Aeronautics and
Space Administration

**Lyndon B. Johnson Space Center**
Houston, Texas

NASA Technical Memorandum 102155

# Orbital Debris Research at NASA Johnson Space Center, 1986 - 1988

Edited by

Robert C. Reynolds, Ph.D.
*Lockheed Engineering and Sciences Company*
*Houston, Texas*

Andrew E. Potter, Jr., Ph.D.
*Lyndon B. Johnson Space Center*
*Houston, Texas*

CONTENTS


| Section | Page |
|---|---|
| ACRONYMS/ABBREVIATIONS | ix |
| ABSTRACT | 1 |
| INTRODUCTION | 1 |
| UPDATE OF THE SPACECRAFT DESIGN ENVIRONMENT (NASA TM 100 471) | 2 |
| DEBRIS POPULATION MODELING | 3 |
| PROGRAM EVOLVE | 3 |
| OTHER LONG-TERM FLUX MODELS | 3 |
| FLUX DIRECTIONALITY MODEL | 5 |
| FLUX IMMEDIATELY AFTER BREAKUP | 5 |
| BREAKUP MODELS | 6 |
| BREAKUP CLASSIFICATION | 7 |
| ORBIT PROPAGATORS | 10 |
| TRAFFIC MODELS | 11 |
| DEBRIS CONTROL | 11 |
| DEBRIS MEASUREMENTS | 12 |
| GROUND-BASED OPTICAL DATA ACQUISITION | 13 |
| The LENZAR Telescope | 13 |
| Socorro Project | 15 |
| Simultaneous Visible/Infrared Observations | 15 |
| Image Processing Facility | 15 |
| GROUND-BASED RADAR DATA ACQUISITION | 16 |
| INFRARED ASTRONOMICAL SATELLITE (IRAS) | 17 |
| MICROPARTICLE DEBRIS STUDIES | 18 |
| Spacecraft Windows | 18 |
| Solar Maximum Satellite Returned Surfaces | 19 |
| PALAPA Satellite Returned Surfaces | 20 |
| Other Microparticle Laboratory Studies | 21 |
| Facility for the Optical Inspection of Large Surfaces (FOILS) | 21 |
| SEM Laboratory | 22 |
| DEVELOPMENT OF DEBRIS MEASUREMENT CAPABILITIES | 22 |
| FLIGHT EXPERIMENT - PHASE A FEASIBILITY STUDY | 23 |
| A PORTABLE CCD DEBRIS TELESCOPE | 24 |
| DEBRIS ENVIRONMENT CHARACTERIZATION RADAR (DECR) | 25 |
| SMART CATALOG PROGRAM | 25 |
| SHIELDING AND VULNERABILITY RESEARCH | 25 |
| HYPERVELOCITY IMPACT MODELING | 25 |
| HYPERVELOCITY IMPACT STUDIES | 27 |
| HYPERVELOCITY IMPACT RESEARCH LABORATORY (HIRL) | 28 |
| REFERENCES | 30 |

## TABLES


| Table | | Page |
|---|---|---|
| 1 | CLASSIFICATION OF DEBRIS BREAKUP: BREAKUP OF KNOWN CAUSE[9]- POSTERIOR PROBABILITY OF MEMBERSHIP IN TYPE | 9 |
| 2 | CLASSIFICATION OF DEBRIS BREAKUP: BREAKUP OF UNKNOWN CAUSE[9]- POSTERIOR PROBABILITY OF MEMBERSHIP IN TYPE | 9 |
| 3 | EPISODIC DATA FROM IRAS COMPARED TO RANDOM NOISE | 18 |
| 4 | CRITICAL REQUIREMENTS FOR GROUND-BASED DEBRIS RADAR (NEEDED TO SUPPORT SPACE STATION DESIGN) | 26 |
| 5 | BASELINE RADAR PRIMARY CHARACTERISTICS | 27 |


## FIGURES


| Figure | | Page |
|---|---|---|
| 1 | Orbital Debris Project organization | 33 |
| 2 | Current flux[2] compared to existing orbital debris measurements | 34 |
| 3 | Debris flux versus altitude for 1995 compared to January 1989 catalogued environment[3] | 35 |
| 4 | Distribution in relative impact velocity for a spacecraft in 28-1/2°, 500 km orbit | 36 |
| 5 | Debris flux from objects with diameter 4 mm or greater at 500 km altitude with different increases in rate of yearly traffic input | 37 |
| 6 | Logic structure in PROGRAM EVOLVE | 38 |
| 7 | Flux versus altitude for the current tracked population (top plot) and for intact objects (lower plot) from PROGRAM EVOLVE | 39 |
| 8 | Debris population growth rate versus population size for best estimate values of A, B, and C for the current population | 40 |
| 9 | Population growth using a simple particle-in-box model for 2 percent growth in launch rate through 2020, constant launch rate thereafter | 41 |
| 10 | The penetration pattern for the 100 largest objects in a standard breakup through planes 20°, 90°, and 170° downrange from the breakup point | 42 |
| 11 | Collision probability for a 250 $m^2$ spacecraft passing through the center of a debris cloud as a function of distance downrange of the breakup | 43 |
| 12 | Breakup plot for the baseline breakup model | 44 |
| 13 | Fragment number distribution versus size for the SOLWIND breakup | 45 |
| 14 | Orbital debris light curve from LENZAR observations | 46 |
| 15 | IRAS constant range contours | 47 |

16 Solar Maximum flux values derived from holes and craters in the thermal control louvers ..... 48
17 Artist's concept for a space-based debris telescope ..... 49
18 Alternative all-reflecting Schmidt designs for a space-based debris telescope ..... 50
19 The portable ground-based CCD telescope ..... 51
20 A radar system, similar in size to the DECR, being used in a zenith starring mode ..... 52

## ACRONYMS/ABBREVIATIONS

| | |
|---|---|
| AFSPACECOM | Air Force Space Command |
| AGK3 | Astronomisch Gesellschaft Katalog |
| ALTAIR | Long Range Tracking and Instrumentation Radar |
| AMOS | Maui Optical Station |
| CCD | Charged Coupled Device |
| CDR | Critical Design Review |
| CNDB | Civil Needs Database |
| DARPA | Defense Advanced Research Projects Agency |
| DECR | Debris Environment Characterization Radar |
| DoD | Department of Defense |
| EDS | Energy Dispersive Spectrometer |
| EVA | Extravehicular Activity |
| FLTEX | Flight Experiment |
| FOILS | Facility for the Optical Inspection of Large Surfaces |
| GEODSS | Ground-Based Electro-Optical Detector System |
| GRC | General Research Corporation |
| GTO | Geosynchronous Transfer Orbit |
| HIRL | Hypervelocity Impact Research Laboratory |
| HVET | High Velocity Electrothermal |
| IRAS | Infrared Astronomical Satellite |
| JSC | Lyndon B. Johnson Space Center |
| LEO | Low Earth Orbit |
| LESC | Lockheed Engineering and Sciences Company |
| LIPS | Library of Image Processing Software |
| LPI | Lunar and Planetary Institute |
| LSPI | Large Scale Programs Institute |
| MIT | Massachusetts Institute of Technology |
| MOTIF | Maui Optical Tracking and Identification Facility |
| NASA | National Aeronautics and Space Administration |
| NTSC | National Television Standards Committee |
| NAVSPASUR | Naval Space Surveillance System |
| OAST | Office of Aeronautics and Space Technology |
| PARCS | Perimeter Acquisition Radar Attack Characterization System |
| PC | Personal Computer |

| | |
|---|---|
| PTTD | Photography and Television Technology Division |
| RCS | Radar Cross-Section |
| REDRAD | Reentering Debris Radar |
| SAO | Smithsonian Astronomical Observatory |
| SDIO | Strategic Defense Initiative Office |
| SEM | Scanning Electron Microscopy |
| SMM | Solar Maximum Mission |
| SRM | Solid Rocket Motor |
| STEM | Scanning Transmission Electron Microscope |
| STS | Space Transportation System |
| TEM | Transmission Electron Microscope |
| USSPACECOM | United States Space Command |
| VDAS | Video Data Analysis System |
| WORM | Write Once, Read Only |

## ABSTRACT

Research on orbital debris has intensified in recent years as the number of debris objects in orbit has grown. The population of small debris has now reached the level where orbital debris has become an important design factor for the Space Station. The most active center of research in this field has been the NASA Lyndon B. Johnson Space Center (JSC). Work has been done on measurement of orbital debris, development of models of the debris population, and development of improved shielding against hypervelocity impacts. Significant advances have been made in these areas, and the purpose of this document is to summarize these results and provide references for further study.

## INTRODUCTION

The orbital debris program at JSC incorporates the efforts of a number of individuals within NASA and various contractor support organizations. The onsite support contractor for NASA is Lockheed Engineering and Sciences Company (LESC), and most contractor support is provided through LESC subcontracts. During 1986-1988 subcontracts were placed with Teledyne Brown Engineering, General Research Corporation (GRC), University of Arizona, University of Colorado, University of Texas, Photometrics Ltd , Spectrometrics Incorporated, Optomechanics Research Incorporated, Astronautics Corporation of America, Eagle Engineering Incorporated, Southwest Research Institute, System Planning Corporation, and the Large Scale Programs Institute (LSPI).

The debris program activities have been organized into the areas of modeling, debris measurements, development of debris measurement capabilities, and shielding and vulnerability research. A particularly important modeling task during this period was an update of the spacecraft design environment. Debris measurements are being made at an increasing rate and are providing data needed in the modeling work, which provides assessments of current and future hazard levels, evaluates response alternatives, and defines requirements for additional data. There is a continuous process of evaluating requirements for new instruments and new laboratory facilities to fill data gaps and provide higher quality data. Several laboratories provide institutional support for many projects. Figure 1 provides the organization of activity within the program and indicates individuals and organizations that are involved in various projects.

Data are acquired with optical (visible and infrared) and radar instruments for large ($>10$ cm) objects, visible optical alone for slightly smaller ($>5$ cm) exposed surfaces for microparticle ($<300$ micron) objects, and from laboratory experiments in the Hypervelocity Impact Research Laboratory (HIRL) and the Scanning Electron Microscopy (SEM) Laboratory. An Image Processing Facility, housing the Video Data Analysis System (VDAS), is a third support facility. An optical laboratory and a radar processing laboratory are planned. Three major instrument development projects - a charged coupled device (CCD) ground-based debris telescope project, a flight experiment feasibility study, and the debris environment characterization radar (DECR) project - were started in 1988.

## UPDATE OF THE SPACECRAFT DESIGN ENVIRONMENT (NASA TM 100 471)

Since the publication of the first Space Station design environment (JSC 20001)[1], new data have been obtained from the Solar Maximum satellite returned surfaces, Socorro ground-based telescopes, and Department of Defense (DoD) radars. The debris flux implied by these data is summarized in figure 2. Also, new data have been collected on breakups, and new evolution models have been developed for debris in low Earth orbit (LEO). All of this information has been incorporated into an update of JSC 20001; this document is currently being reviewed prior to official release[3]. There are three parts to the document:

a. Definition of the debris background spatial flux values as a function of debris size, orbital altitude, solar flux at 10.7 cm, and time

b. Definition of encounter geometry distribution based on orbital characteristics of tracked debris objects

c. Definition of flux contributions from individual breakup events

The background flux was defined by analyzing historical data to develop functional forms to predict future debris fluxes. These data were fit to functional forms in size, altitude, solar flux, and time. For trackable debris, flux levels are inversely proportional to atmospheric density (with a 1-year time delay) up to 500 km altitude. Above that altitude there is very little removal by atmospheric drag. Although flux levels below 500 km are sensitive to solar activity, the trend in the update is to exceed the predictions of JSC 20001 by the year 1995. The background flux as a function of altitude is shown for the year 1995 in figure 3.

The distribution of encounter geometries for collision between a spacecraft and a debris object was modeled using tracked objects from the United States Space Command (USSPACECOM) catalog. The encounter geometry distribution varies with the spacecraft orbit and the location within the orbit. As might be expected, the encounters were found to be concentrated near the local horizontal plane for circular mission orbits. Encounters cover an increasingly large solid angle as maximum impact velocity is reduced, but the likelihood of encounter also decreases; only approximately 1 in 1000 encounters will have impact velocity less than 1 km/sec. The same distribution of encounter geometries will be exhibited for the small, unobserved debris if this material has the same distribution in semi-major axis, eccentricity, and inclination as the tracked debris. Inclination distribution is by far the most important, and untracked debris could be expected to have an inclination distribution similar to the tracked debris. The distribution of impact velocities for a spacecraft in a 28.5°, 500-km orbit is shown in figure 4.

Debris clouds from breakup events in orbit are growing in importance as temporary contributors to the catalog. Therefore, the role of individual breakups was discussed in the update, and a functional form for the change of spatial density in the cloud with debris size, altitude, solar activity, and time was provided.

## DEBRIS POPULATION MODELING

The two primary modeling efforts are hypervelocity impact modeling and debris population modeling, which include analysis of data, population evolution modeling, and assessment of effectiveness of debris control options. Comprehensive spacecraft vulnerability modeling, which includes assessment of design options, failure modes and effects of analysis, and feedback into the defined threat, is only beginning to be developed at JSC.

The first long-term population evolution model was proposed by Reynolds and co-workers at the JSC orbital debris workshop in 1982[4]. Early work in this area at JSC was performed by Kessler and Su. Using an approach that followed the "average" or expected growth in the debris population, Su was able to point out as highly nonlinear the relationship between the increase in future space traffic and the flux of debris objects, a state driven by the creation of collisional debris fragments[5]. This result is shown in figure 5, taken from that reference. The average model was a very useful first generation approach, but it was extremely computer intensive, lacked the ability to use detailed mission models in its future projections, and did not fully account for the stochastic nature of future projections. In 1988, the decision was made to replace it with a new type of model, embodied in a program named EVOLVE.

A number of support models has been developed as a part of the debris population modeling effort. These are discussed individually. Figure 6 shows the organizational structure for these models and their relationship in the evolution code. The models have been designed to function as independent elements as well as to serve as modules for the evolution code.

## PROGRAM EVOLVE

A new debris evolution model, PROGRAM EVOLVE, is being developed. In this model there are two types of entities - intact objects and debris clouds. Intact objects arise from launch or normal space operations; the orbits of these objects evolve deterministically. Debris clouds arise from on-orbit collisions or explosions, and evolve using a phenomenological model for the change of debris flux as a function of altitude, solar activity, and time. The options of developing either a Monte Carlo model or an average growth model from this concept are being evaluated.

The first test of the program will be to reconstruct the current population from historical space activity. From 1957 through 1987 there were 18,998 objects placed in orbit, of which 11,794 have been classified as debris and 7,327 as intact objects. Figure 7 shows the population that would have existed if only these 7,327 objects had been placed in orbit, i.e., if no breakups had occurred, compared to the currently tracked populations.

## OTHER LONG-TERM FLUX MODELS

Several flux models have been developed to characterize hazards to spacecraft and to help define requirements for debris observation programs. The projection of background flux as an extrapolation of past space activity, discussed in the section on update of the spacecraft design environment, made

extensive use of historical data. Obviously, such a model is limited in the deviations from past activity that it can support, is not well-suited to analyzing the sensitivity of model predictions to the processes involved in debris growth, and will be untrustworthy for large time extrapolations, particularly if non-linear processes become important. This model will require re-evaluation and updates as changes in traffic models and other new data become available.

A very simple, but interesting model, using only the functional form of the equation for conservation of particle number, was developed which gave insight into debris population stability and equilibrium states for debris. This differential equation may be written as

$$\dot{N} = \frac{dN}{dt} = A + BN + CN^2$$

where

N = number of objects in population
t = time

A, B, and C, which in general will be both space- and time-dependent, may be related to source or sink processes driving population growth or decay. The A coefficient reflects number of independent processes, such as launches, the B coefficient represents number of dependent processes, such as atmospheric decay, explosions, or debris collection, and the C coefficient represents collision processes. The quadratic form of the source terms is sufficient to provide insight into asymptotic debris states demanded by specific choices of A, B, and C.

A reasonable choice for A, B, and C can be made for current practices and current traffic plans. These coefficients are

A = 384 Rationale: Expected traffic rates and launch-associated debris same as historical launches

B = -0.01 Rationale: Reasonable rates of atmospheric drag removal

C = $1.9 \times 10^{-8}$ Rationale: Reasonable choice for collision cross-section

and lead to figure 8, indicating a stable equilibrium point is approximately 40,000 objects, and an unstable point approximately 500,000; that is, the population will want to stabilize at approximately 40,000 objects. We are currently at point $N_c$, and are therefore experiencing a growth in population size, but one that will be bounded.

The above discussion is, of course, not entirely realistic since the coefficients will change in time, but this primitive model does illustrate the general behavior of population growth in time. In particular, it points out that under many conditions, including the present state, there are large, but bounded equilibrium states. However, such states might not be tolerable for conducting space operations.

To add more realism to this model, a simple numerical "particle-in-box" model was developed that allowed the coefficients to change with time, as collisions and explosions altered the size distribution for orbiting objects. The behavior of an "unbounded growth" initial model is seen in figure 9 to have a rapid growth phase, which is cutoff as collisions start to break down large objects more and more rapidly.

## FLUX DIRECTIONALITY MODEL

The expected distribution of impact geometries derived for the tracked population has important application for spacecraft shielding, as discussed in the section on update of the spacecraft design environment. This impact geometry distribution model has also been used to define a debris flux field, which can be used to calculate rates at which debris will cross the field-of-view of debris telescopes or radars.

New types of orbits, for example ballistic trajectories, are being investigated for their directional characteristics. In contrast to near-circular orbits which lead to two hot spots in the local-horizontal plane (for a spacecraft in circular orbits) focussed nearly directly downrange, ballistic trajectories will tend to give hot spots forward focussed, but out of the horizontal plane. This will lead to four hot spots, two below horizontal for impact on the ascending part of the orbit and two above the horizontal as the objects are returning to Earth.

A second interesting case, yet to be addressed, is directionality of debris from a cloud co-moving with a spacecraft. This debris will have a much lower relative velocity and have a much broader angular distribution. An example of such a situation might be the Space Station, in which accidents associated with it as a traffic node, routine operations, and low speed secondary fragments from hypervelocity collisions between the Space Station and small debris in orbit, will create a debris cloud co-moving with the Space Station.

## FLUX IMMEDIATELY AFTER BREAKUP

Modeling of the debris cloud immediately after breakup was begun in an effort to quantify the threat posed to other spacecraft in the environment by such a cloud. The modeling approach is somewhat different than that used by Chobotov and co-workers[6], in that the cloud is characterized by the flux field it generates rather than by a spatial distribution of a number density function. The model has been incorporated into software in PROGRAM CLOUD.

This program has several uses. It accesses a user-defined breakup model to provide initial conditions for a set of debris fragments defined by the user. So far, only a standard collisional breakup model has been used. These initial conditions are cast into USSPACECOM two-card element set format, and have been used to provide element set data for the cloud evolution studies supporting PROGRAM EVOLVE and used by the spatial display program, PROGRAM PIC, to show plot or animated images of cloud development and passage of model fragments across the field-of-view of ground-based sensors.

However, the most important function of this model has been to quantify the debris hazard posed by a debris cloud. This is done by defining the flux field generated by the debris particles through reference plane oriented normal to the unperturbed orbital plane at various distances downrange. A satellite is then flown through this flux field and collision probability calculated. Three examples of the penetration pattern through reference planes 20°, 90°, and 170° downrange of breakups are shown in figure 10. It should be remembered that these objects penetrate the planes at different times. These objects consist of the 100 largest objects in the standard breakup, and consist of objects to approximately 20 cm in diameter or larger. Extending the calculation to objects 10 cm in size or larger, and flying a 250 $m^2$ spacecraft (Shuttle-sized) through the center of the cloud leads to collision probabilities as a function of down-range distance as shown in figure 11. The falloff from 0° through 90° reflects the expansion of the cloud both radially and cross-range; although the cloud contracts in cross-range, it continues to expand radially from 90° to 180°, but since the cloud continues to stretch in the down-range direction throughout, no increase in collision probability is seen. From 180° to 270°, the cloud contracts radially while expanding cross-range. Finally, from 270° to 360°, the cloud contracts both radially and cross-range. At this point, a rise in flux is observed, as might be expected, but not nearly to the levels near breakup; the cloud has experienced a significant expansion in the down-range dimension during this first revolution.

The roughness of the plot is probably not real, but rather a reflection of the fact that the volume of the cloud has gotten large enough that the number of fragments used to define the flux was not large enough. For smaller fragments, this situation will get worse, as the cloud volumes are larger

## BREAKUP MODELS

Several ground-based tests and on-orbit breakups have provided data for the current baseline breakup model. The distribution of delta-v vs. fragment size is taken to have the functional form first suggested by Su[7] of

$$log(dv_{peak}) = \begin{cases} a_o + a_1 (log \frac{d}{d_m})^2 & d \geq d_m \\ a_o & d < d_m \end{cases}$$

where

$a_o$ = 0.875
$a_1$ = -0.0676
$d_m$ = $9.9083 \times 10^{-8}\ m_p^{1/3} v_p^{2/3}$ (m)
$m_p$ = projectile mass (kg)
vp = projectile impact velocity (km/sec)

and where $dv_{peak}$ is the most probable delta-v for that size. For $m_p$ = 15 kg and $v_p$ = 10 km/sec, $d_m = 1.24 \times 10^{-6}$ m.

A triangular spreading function ramping up from 0 at delta-v = $0.1 \cdot dv_{peak}$ to maximum at $dv_{peak}$ and then ramping back to 0 again at $1.3 \cdot dv_{peak}$ is imposed upon this distribution. This spreading function simulates the spread in velocity perturbations encountered for fragments of a given size during a breakup.

There is better data on fragment size distribution than on velocity distributions. In keeping with the functional form suggested by Bess[8], a size distribution can be defined for explosions and for collisions. The distributions are taken to be

$$N(m) = \begin{cases} 0.4478 \left( \dfrac{m_T}{m_p v_p^{\,2}} \right)^{-0.7496} & \text{collisions} \\ \left. \begin{array}{ll} 1.707x10^{-4} m_T \; EXP\left( -0.0206 \sqrt{m} \right) & m \geq 1.94\ kg \\ 8.692x10^{-4} m_T \; EXP\left( -0.0576 \sqrt{m} \right) & m < 1.94\ kg \end{array} \right\} & \text{explosions} \end{cases}$$

where

| | | |
|---|---|---|
| N(m) | = | number of objects of mass m, in grams, or larger |
| $m_T$ | = | mass of exploding object |
| $v_p$ | = | projectile impact velocity (km/sec) |

Fragment diameter, d, in meters, is related to fragment mass, m, in grams, by

$$m = \begin{cases} 4.72x10^{4} \; d^{2.26} & d \geq 0.01\ m \\ 1.40x10^{6} \; d^{3} & d < 0.01\ m \end{cases}$$

A breakup plot for the 100 largest fragments of a collisional breakup with $m_p = 15$ kg and $v_p = 10$ km/sec is presented in figure 12. Laboratory data on hypervelocity impact into structures and element set data for actual breakups and modifications to these baseline breakup equations are expected to be made in the next year.

## BREAKUP CLASSIFICATION

Historical data sets for the 26 largest breakups have been analyzed to better understand on-orbit breakup processes. Element sets from specific breakups have been analyzed for characteristics indicating the cause of the breakup, and breakup fragments have been analyzed for area-to-mass values based on decay characteristics. Radar cross-section data, which are related to cross-section area, have been combined with area-to-mass values to derive fragment masses.

The development of breakup signatures from analysis of breakup events of known cause has been discussed by Badhwar and co-workers[9]. After examining a number of breakups and many characteristics of those breakups, it was determined that fragment size distribution and plane change angle present such signature information. Fragment size distributions were found to fit a function of form

$$\frac{dN}{dr} = K_o r^{\alpha} \, EXP\left( - \frac{\alpha}{\gamma} \left( \frac{r}{R_m} \right)^{\gamma} \right)$$

where $\alpha$, $R_m$, and $\gamma$ are distribution parameters. A plot of some typical data with the functional fit is shown in figure 13. The $\alpha$ parameter characterizes the rising slope to the left, $R_m$ the peak in the distribution, and $\gamma$ the falloff of the function on the right. Plane change angle distributions were found to fit a normal distribution plus a constant background, thus,

$$\frac{dN}{d\Theta} = \frac{K_1}{\sigma} \quad EXP\left( - \frac{(\Theta - \Theta_p)^2}{2\sigma^2} \right) + \eta$$

It was assumed that on-orbit breakups occurred from low intensity or high intensity explosions, or from collisions. High intensity explosions result from explosive materials being in contact with the spacecraft structure. Low intensity explosions are conflagrations, explosive decompression, or other events characterized by a gas-pressure wave passing through the structure. A set of breakups were treated as being of known cause; those breakups were analyzed to produce quantities correlating to breakup cause. These quantities were then derived for breakups of previously unknown cause to attribute cause in those cases.

After performing a sensitivity test for the distribution parameters on known breakups, the most important parameters were found to be $R_m$, $\gamma$, and $\sigma$. A linear classifier was trained on the known breakup events using these three parameters to define a discrimination function, and this function was used to classify breakups of unknown origin. Table 1 presents the known breakups with classification and table 2 the classification of unknown breakups.

TABLE 1.- CLASSIFICATION OF DEBRIS BREAKUP: BREAKUP OF KNOWN CAUSE[9]- POSTERIOR PROBABILITY OF MEMBERSHIP IN TYPE

| Satellite | Known type | Classified into type | C | D | E |
|---|---|---|---|---|---|
| COSMOS 839 | C | C | 0.6031 | 0.0000 | 0.3969 |
| SOLWIND | C | C | 0.9185 | 0.0000 | 0.0815 |
| COSMOS 1375 | C | C | 0.6988 | 0.0000 | 0.3012 |
| HIWARI | D | D | 0.0000 | 1.0000 | 0.0000 |
| LANDSAT 1 | D | D | 0.0000 | 1.0000 | 0.0000 |
| LANDSAT 3 | D | D | 0.0000 | 1.0000 | 0.0000 |
| NOAA 3 | D | D | 0.0000 | 1.0000 | 0.0000 |
| NOAA 4 | D | D | 0.0000 | 1.0000 | 0.0000 |
| NOAA 5 | D | D | 0.0000 | 1.0000 | 0.0000 |
| LANDSAT 2 | D | D | 0.0605 | 0.9034 | 0.0361 |
| COSMOS 252 | E | E | 0.3228 | 0.0000 | 0.9772 |
| COSMOS 970 | E | E | 0.0826 | 0.0000 | 0.9174 |
| COSMOS 886 | E | E | 0.2141 | 0.0000 | 0.7858 |
| COSMOS 397 | E | E | 0.4724 | 0.0000 | 0.5276 |
| COSMOS 375 | E | C * | 0.6205 | 0.0000 | 0.3795 |
| COSMOS 374 | E | E | 0.2166 | 0.0000 | 0.7834 |

*Misclassification observation (probably due to mixing of COSMOS 374 and COSMOS 375 orbital elements)

C - Hypervelocity impact

D - Low intensity explosion

E - High intensity explosion

TABLE 2.- CLASSIFICATION OF DEBRIS BREAKUP: BREAKUP OF UNKNOWN CAUSE[9]- POSTERIOR PROBABILITY OF MEMBERSHIP IN TYPE

| Satellite | Classified into type | C | D | E |
|---|---|---|---|---|
| ARIANE | E | 0.2142 | 0.0000 | 0.7858 |
| COSMOS 1275 | E | 0.3813 | 0.0000 | 0.6187 |
| COSMOS 61-63 | E | 0.3147 | 0.0000 | 0.6853 |
| NIMBUS 4 | C | 0.9328 | 0.0000 | 0.0672 |
| OPS7613 | D | 0.0000 | 1.0000 | 0.0000 |
| TITAN 3C | C | 0.8198 | 0.0000 | 0.1802 |
| TRANSIT | C | 0.8816 | 0.0005 | 0.1178 |
| COSMOS 1461 | C | 0.5510 | 0.0000 | 0.4490 |
| COSMOS 1220 | E | 0.1358 | 0.0000 | 0.8642 |

Approximately 2600 fragments from 24 breakups having element sets available for at least 3 years have been analyzed for area-to-mass characteristics[7], with the objective of determining the mass of the objects given their observed radar cross-section (RCS). Before examining debris fragments, this work was calibrated using 196 intact objects of known size, shape, and mass. For the intact objects, the best power law fit for the relationship between RCS and mean cross-sectional area, A, was determined to be

$$A = 0.5712 \ RCS^{0.7666}$$

For the intact objects, this led to a fit consistent with previous work[8], and for debris, led to the conclusion that the mean mass, m, can be related to mean area, by the relation $m \alpha A^{1.86}$, although for a given area the mean mass distribution can be very broad.

A project is also in progress to determine the velocity perturbation characteristics experienced by fragments during breakup. Although results are only preliminary, several breakups have been analyzed and indicate very reasonable perturbation characteristics. We expect to have the technique ready for publication before the end of 1989.

There has also been a long-term project to collect and analyze data on breakups as soon as they are identified by the DoD radars. This activity has been documented in a periodically updated history of on-orbit satellite fragmentations[9].

## ORBIT PROPAGATORS

Both long- and short-term propagators are used to update debris orbits. Long-term propagators have been used primarily to calculate drag rates for objects in LEO for evolution modeling, whereas short-term propagators have been used to support debris observation programs and to investigate deterministic interactions between a spacecraft and the debris environment.

The most extensively used long-term propagator has been a model developed by Mueller[13] that accounts for atmospheric drag and for lunar and solar perturbations.

An historical investigation of orbit decay for a number of breakups and intact objects was conducted by Hoots and co-workers at GRC. Using a Jacchia atmospheric model and observed radar cross-sections, an improved ballistic coefficient model was developed[14]. This work offered an opportunity to compare theoretically derived ballistic coefficients with empirically derived ballistic coefficients for a large number of known objects in orbit. GRC also conducted a project to make element sets generated by the Naval Space Surveillance System (NAVSPASUR) and USSPACECOM astrodynamically compatible[15]. Once this capability is integrated into the USSPACECOM system, it will reduce the burden on uncorrelated target analysis and reduce the number of analysis satellite element sets. It will also make it easier at JSC to derive time and location of breakups when fragmentations occur in orbit.

A set of short-term propagators are available in the SATRAK software package being developed by Grissom and co-workers at Teledyne-Brown Engineering to address problems associated with satellite tracking. USSPACECOM's SGP4 propagator has been used most extensively in the debris program,

but other propagators are available in this package. The SATRAK software is user-interactive and provides a wide range of analysis capabilities, featuring both tabular and graphical output[16].

## TRAFFIC MODELS

A number of traffic models has been developed to address specific modeling requirements. For testing the new evolution model, the historical traffic from 1957 through 1987 has been put into a database. The predicted traffic for the United States has been defined using NASA's Civil Needs Database (CNDB) and various contractor-defined Space Station infrastructure models. Traffic from non-United States programs has been predicted using growth parameters derived from historical activity. Alternate forms of these traffic models, or parts of them, can be defined and the resulting files concatenated to constitute a traffic model suitable for use in evolution modeling. Support software is being prepared to provide a report of the mission model characteristics in a report form suitable for inclusion in documentation of the modeling effort.

The LSPI of the University of Texas at Austin provided NASA support by acting as a technical/ managerial liaison between NASA and the Strategic Defense Initiative Office (SDIO) and by providing software development and integration. LSPI personnel actively participated in the development of appropriate mission (or traffic) models for inclusion in NASA's orbital debris population evolution program. These models, and an associated operating system shell, not only account for manifested traffic to orbit, but also include logistical concerns such as rocket booster, servicing, and payload retirement requirements. This capability will allow the debris community and other interested parties to perform trade studies on debris evolution and/or mitigation, using the best available prediction of future space traffic. LSPI has worked actively to develop interfaces with NASA software, and to run their combined NASA/LSPI system in both single-user machine (e.g., COMPAQ) and multiuser machine (e.g., VAX) environments.

## DEBRIS CONTROL

The issue of control measures to regulate debris hazard has been an ongoing subject of concern. Removal of hardware from the environment before breakups can occur, either by preplanned onboard operations or by rendezvous and retrieval, as well as for removal of material once it has fragmented[17], are options that have been investigated.

Removal of large objects before they fragment was found to be the most effective and least expensive means of control. Below approximately 700 km this could reasonably be achieved by drag augmentation, e.g., through the use of balloons that would inflate at the end of the operational life of the space hardware in question. Above this altitude, drag augmentation becomes expensive and propulsive deorbit becomes more economical. In general, very small propulsive burns would be required to lower perigee enough to guarantee rapid reentry. The advantage of preplanned deorbit is that a very simple, low-weight system could be used and represent a minimal cost addition for any program.

The alternative of rendezvous and retrieval in LEO is expensive because orbit plane orientations are randomized. Hence, there are large propulsion requirements to move from one orbiting

object to another, although the fuel cost may be reduced by residing in drift orbits between rendezvous maneuvers if the orbits are of nearly the same inclination. At the present time, the NASA version of the orbit maneuvering vehicle may not be suitable for supporting such operations. However, if the need to perform on-orbit servicing develops, an alternative vehicle may emerge.

The alternative of removing fragments and other small objects using debris sweepers has also been investigated. While such a concept is much more expensive, it would allow for the possibility of cleaning up breakup fragments if a breakup did occur, and might be an attractive support capability for major programs such as Space Station. A major problem is to use materials that do not add fragments to the environment while sweeping up debris; foams, dust, and electromagnetic fields have been suggested. For a sweeper to be effective, it need only remove enough kinetic energy to significantly reduce deorbit time. A 2 percent reduction in velocity is sufficient to do this for any object below 1500 km. However, the amount of sweeper material needed to be placed in orbit is very large if a passive sweeper is used and a reasonably short clean out time is desired. Further, such a sweeper would clean out useful payloads as efficiently as it would debris, if these payloads were not equipped to avoid such encounters. An active sweeper system, in which a small collector area is placed in the path of a debris object, might be a feasible sweeper concept from the standpoint of weight-to-orbit, but detection and maneuvering systems would require a major developmental effort.

GT-Devices of Arlington, Virginia, performed a study to examine the use of ground-launched projectiles for on-orbit debris removal[18]. The scheme would utilize a ground-based, vertically-oriented High Velocity Electrothermal (HVET) Gun to launch these projectiles (the HVET Gun is a variant of the so-called rail gun, which accelerates the projectile via plasma pressure). At altitude, the projectile would either convert to an inflated balloon or fragment itself; collision of an on-orbit debris object with either the balloon or the relatively dense debris cloud would tend to decrease the momentum of the debris object and hence lower its perigee. This would promote the objects' early atmospheric reentry. Advantages offered by this technique include low operating cost, since only the projectile itself is incapable of reuse, and a high frequency of projectile launch.

## DEBRIS MEASUREMENTS

The area of most rapid growth during 1986-1988 has been the acquisition of data on orbital debris. To a large extent this has come about because of cooperation with USSPACECOM to use its sensors to acquire and disseminate debris data. More use has been made of ground-based radar data, both by extracting more information from data that were always available and by getting data from special tasking of these sensors. Data from more sensitive telescopes - the USSPACECOM Ground-based Electro-optical Detector System (GEODSS) telescopes at Maui and Diego Garcia - are seeing objects smaller than the radars are cataloging, and the smaller, portable NASA telescope is being used more actively to acquire data for albedo determination. The analysis of Solar Maximum returned surfaces has allowed us to define the small particle end of the debris flux, and led to the surprising conclusion that submillimeter-sized paint flakes constitute a significant component of the man-made debris environment in that size range. Finally, the analysis of Infrared Astronomical Satellite (IRAS) data is in progress; there is information on objects smaller than the catalog in this data, but it is extremely difficult to interpret definitively.

## GROUND-BASED OPTICAL DATA ACQUISITION

There have been three projects acquiring ground-based visible and infrared data. These are the LENZAR project, a small, portable dedicated debris telescope with enhanced low light level television data recording, the Socorro project, which employs binocular 31" telescopes at the Socorro Experimental Test Site run by the Massachusetts Institute of Technology (MIT) Lincoln Laboratory, and visible/infrared data acquisition from a facility on Maui, Hawaii.

Primary objectives of these observation programs have been to measure the debris albedos and reduce the minimum size for which debris data are available. Albedo is important for two reasons. First, if albedo and range are known, the observed brightness determines size. Second, the albedo characteristics of a breakup may contain information on the cause of the breakup. Fragments arising from hypervelocity impact tests of simulated spacecraft have been found to be coated with very dark soot arising from a breakdown of the plastics within the structure. High intensity explosions might also be expected to leave a dark residue on fragments. On the other hand, pressure vessel explosion might be expected to only produce bare metallic surfaces of high albedo. Some observed breakups, e.g., ARIANE V16, are characterized by debris of high albedo, while others, e.g., SOLWIND, yielded very dark debris.

### The LENZAR Telescope

The LENZAR telescope is an 8" aperture catadioptric optical system with a 1.9° by 2.1° field-of-view and a low-light level video sensor system. It has been used in three campaigns - in June 1986 in Oregon, to observe debris associated with the breakup of the SOLWIND satellite; in January 1987 in New Zealand, to observe fragments from the ARIANE V16 third stage that broke up in Sun-synchronous orbit, and in July 1987 and July 1988 at Rattlesnake Mountain Observatory in Washington, to observe ARIANE and SOLWIND debris once again and to observe fragments from various COSMOS breakups. Observing campaigns will continue to be scheduled, now with LENZAR and in the future with a new 12.5-inch CCD telescope, so that debris fragments can be intensively observed as soon after breakup as possible.

The limiting magnitude for LENZAR is approximately 12.5 for a stationary image; for debris moving at 0.5 deg/sec through the field-of-view, the limiting magnitude is 10.0. Assuming a Lambert spherical object with albedo of 0.3, this translates into a limiting diameter of 35 cm at 1000 km range and phase angle 90°. By comparing observed brightness with RCS from the USSPACECOM catalog, COSMOS fragments and most other debris are characteristically dark, with albedos typically in the range of 0.03 to 0.3. ARIANE V16 fragments, which have resulted from a low intensity explosion perhaps induced by collision with a small piece of debris, are characteristically brighter, with albedos ranging from 0.1 to 0.8[19]. The RCS values used to derive these albedos have been corrected to account for the error factor of 1.7 found in the Eglin RCS processing. However, a significant uncertainty in the calculation of albedo by this method remains the complex and poorly understood relationship between RCS and physical size that exists for debris.

In comparing breakups of different ages and observing the same fragments over time, it might be expected that dark debris tends to lighten with time and light debris tends to darken. The data acquired thus far are insufficient to confirm this hypothesis, however. More certain is that the debris tumble rates, as inferred from light curves, are more rapid in debris from more recent breakups than from older breakups.

To support the LENZAR project by providing accurate look-angles and appearance times for candidate debris objects, the orbital element set tapes produced on a monthly basis by USSPACECOM were found to be inadequate because the element sets were too old. Therefore, a system of updating element sets three times weekly using element set transmissions from USSPACECOM to Goddard Space Flight Center and electronically forwarded to JSC has been installed. The SGP4 propagator is used to propagate the element sets to the observation time, and a look-angle processor is used to provide information on look-angles and times to develop observing schedules. Using this planning software, approximately 70 percent of the objects with RCS values of 1 $m^2$ are observed, but this drops to approximately 30 percent of the objects having RCS values of 0.5 $m^2$.

A system for data analysis has been installed in the Image Processing Facility to read pixel values for the debris streaks and background stars to provide photometric information from the video data. Photometric calibration stars are obtained from the astronomical selected areas and from the Hubble Space Telescope guide-star catalogs. Our working subset of this last catalog contains only a 1.5° band of the sky centered on 33° declination to support the Socorro project. The Smithsonian Astronomical Observatory (SAO) catalog and the Astronomisch Gesellschaft Katalog (AGK3) are used for field identification.

Two software packages have been written to process the data. Both packages provide sophisticated reduction and analysis techniques, but rely on a user to view the data as tney are being processed and to make decisions on what parts of the video image are to be digitized. The first of these programs extracts digital data from the position and intensity values of debris moving across the field-of-view. It provides light curves and positional information for debris exhibiting time-varying brightness and provides accurate mean magnitudes for debris having constant brightness. Besides digitizing the data for storage in the computer, the program removes the sky contribution to the brightness. A second program has been developed to measure the brightness of stationary images (stars) needed for photometric calibration. A typical, complex light curve is shown in figure 14.

Using this system, approximately 25 nights, each approximately 6 hours in length, have been processed. Each hour of observation yields approximately five debris objects, so that approximately 750 debris streaks have been analyzed. Besides the intended targets, interlopers are also seen. When the selected areas are being observed, the interloper rate is approximately 1 per 40 minutes, which is consistent with the random background predicted from the radar data. However, when the telescope is set to observe a debris object from a relatively new breakup, the interloper rate is approximately 1 per 15 minutes, consistent with many debris objects being a part of a debris cloud, and therefore lying in a region of higher debris density than the general background.

Socorro Project

Two projects have been supported to obtain data from the 31" telescopes at the MIT Lincoln Laboratory's experimental test site facility in Socorro, New Mexico. These telescopes are used to develop and test new capabilities of the GEODSS instruments[20], and operate to a limiting magnitude of 16.5 for stationary images, 13.4 for images crossing the focal plane at 0.5°/sec, and 12.5 for images moving 1.1°/sec. They feature a variable diagonal field-of-view from approximately 0.5° to 1°. Nine hours of data were obtained in 1984 and 35 hours of data in 1985-1987. The first set of data provided information on the debris population to > 5 cm in diameter and indicated a flux greater than that predicted from the radar data. The second set of data is only now being analyzed.

Simultaneous Visible/Infrared Observations

Simultaneous visible and infrared observations have been acquired using instruments at the Defense Advanced Research Projects Agency (DARPA), Maui Optical Station (AMOS), and the Maui Optical Tracking and Identification Facility (MOTIF), and preliminary results are coming out of these data[21]. The data indicate a slow cooling of debris upon entering the Earth's shadow and an increase in temperature upon reemerging into the Sun. Although the debris pieces slowly rotate, in general, they are not longitudinally isothermal. The derived albedos are low, consistent with the optical observations. Observation of spherical standards led to a factor of two error in derived versus actual diameter.

During FY88 a subcontract was established with the University of Arizona for the services of Dr. Larry Lebofsky to engage in a study of thermal models applicable for visual and infrared studies of orbital debris. This research is directly applicable to the concerns of the orbital debris flight experiment both in assessing optimum modes of observing and in the interpretation of simultaneously made visual and infrared observations.

Image Processing Facility

The VDAS consists of the Gould IP8500 image processing system, a DEC Micro-Vax II host computer with peripherals, and an Eikonix image digitizing scanner. The Gould system can be configured as a single 1024-line system or as two 512-line resolution workstations. The Gould system includes 16 memory planes, a high-speed warper and histogrammer, and an auxiliary graphics processor. Each workstation has a color monitor, a trackball interactive control device, and a DEC VT240 terminal for software control. The image processing software used is primarily Gould's library of image processing software (LIPS) plus additional functions programmed at the Lunar and Planetary Institute (LPI) and by VDAS programmers. The Gould system also includes three video analog-to-digital converters capable of digitizing a standard NTSC television signal (monochrome and color) and a real-time disk system which can store 800 512-by 512-by 10-bit images at 30 frames per second (television rate). The computer system consists of a DEC Micro-VAX II with nine megabytes of memory and an RA-81 456-megabyte disk system running under a VMS 4.6 operating system. Two RA-60 200-megabyte removable disk pack storage devices are used for storage of image data.

Peripheral devices include a system console (LA100), an LA210 printer, a TS05 nine-track tape unit, a quad-density (800 to 6250 bpi) tape drive, a TK-50 cassette tape unit, two optical laser write once, read many (WORM) drives which provide 1.6 gigabytes of online removal storage, a high-speed streaming tape backup system which facilitates system backups, and four VT240 terminals (including the two at the Gould workstations). The Eikonix scanner can be allocated to either workstation to digitize an image under user control at user selectable resolutions of up to 2048 by 2048 pixels. A matrix camera can record, on either 35 mm or 8 by 10 color film, any low-resolution color video image being displayed on either workstation. Eight-by ten-inch images may also be printed using the D-SCAN CH-5301 color printer. Precision film recording is done by writing the red, green, and blue color channels to computer tape and film recording them on the Optronics C-4300 colorwriter at the LPI. A capability to output the images viewed on the Gould monitors as National Television Standards Committee (NTSC) color video also exists.

A fiber optic cable interface to the NASA television system has been installed by the Photography and Television Technology Division (PTTD) to link VDAS with video data from any of NASA's sources. This enables the VDAS to broadcast and receive television data through PTTD.

## GROUND-BASED RADAR DATA ACQUISITION

Besides the radar-based element set data provided by USSPACECOM, special tasking has provided data acquired by the Kaena Point radar in Hawaii, the Perimeter Acquisition Radar Attack Characterization System (PARCS) in North Dakota, the FPS-85 at Eglin AFB, Florida, and the DARPA Long Range Tracking and Instrumentation Radar (ALTAIR) System at Kwajalein. The small satellite tests conducted by PARCS have been reported elsewhere[22]. Kaena Point radar data were acquired in connection with AMOS/MOTIF observations. In the future, more radar special tasking will be requested to improve our understanding of RCS and to acquire data on breakups.

There is typically a several month delay between the occurrence of a breakup in orbit and the appearance of fragments identified with the breakup in the satellite catalog. By the time this occurs, much useful information on the breakup has been lost; for example, in the breakup of the 1986-069 satellite, there is early radar data indicating at least 450 objects in the debris cloud, but only 16 of these objects were finally catalogued. In consequence, there is an ongoing program, performed with Teledyne-Brown Engineering, to notify NASA as soon as a breakup is detected, and to acquire whatever data are available on the breakup. There are currently plans to request a more formal and extensive collection of breakup data and to systematize the flow of that data to NASA for analysis.

Since the breakup of the ARIANE V16 (SPOT-1/VIKING) rocket body in Sun-synchronous orbit and the indication of other debris in a 7° geosynchronous transfer orbit (GTO), JSC has routinely requested special tasking and reports of information acquired from DoD radars on the upper stages and payloads associated with each subsequent ARIANE launch. Since that activity has been initiated, V19 has given evidence of a shedding of material, perhaps thermal insulation, in GTO. The ARIANE V20 launch experienced anomalies in the deployment of the solar panels on the West German TVSAT payload, and the rocket body may have experienced anomalous reentry on its first perigee passage. The stage did pass through the COSMOS 1646 fragment cloud. There were indications in the tracking data that the upper stage was experiencing anomalous thrust throughout its first pass in GTO, but the evidence is not conclusive.

A dedicated debris radar system, the reentering debris radar (REDRAD), is currently being developed by NASA. This long wavelength (6 meter) radar detects the ionization trail associated with objects entering the upper atmosphere, rather than tracking the debris object itself. Masses for entering particles can be determined with techniques similar to those used in meteor studies[23] by functionally relating the radar measurable parameters of the ionization trail to characteristics of the parent body[24]. Although there is some question as to the minimum size fragment that can be observed with this system, it is predicted that fragments less than 1 centimeter in size (or approximately 1 μgram) can be seen. Although the radar has been used in association with particular breakup events, a data processing system is now being developed to use the radar for longer term monitoring of the environment by observing reentry events from the background population.

## INFRARED ASTRONOMICAL SATELLITE (IRAS)

The IRAS satellite was a liquid helium cooled orbiting infrared astronomical telescope having a 60 cm aperture and 63.6 arcminute field-of-view. The focal plane contained sensors centered on 12, 25, 60, and 100 microns in a two-dimensional masked array. Because of its relatively large aperture and high level of sensitivity, the data returned by IRAS was expected to contain the first information on orbital debris in the millimeter to centimeter size regime. These data are being analyzed for debris information at JSC and at the University of Arizona. At JSC, the interest was focused on the smallest debris which was expected to cross the focal plane very rapidly and at all azimuths.

Preliminary results of the JSC analysis have been reported previously[25]. Approximately 83 hours of IRAS data are available for analysis. The observed data are signal strength and time of sensor turn on. What is desired is fragment size and number of objects detected. Debris size can be inferred from signal strength if range can be determined, which may only be done indirectly for IRAS. Assuming the debris populates circular orbits, which is a good assumption for man-made debris, it is possible to define a unique relationship between range, crossing azimuth, and crossing rate, which is shown graphically in figure 15. As can be seen, good range definition, which is needed so that brightness can be related to size, can only be obtained for fast moving streaks. Therefore, an algorithm was developed to scan through the detector turn ons to search for sequences of turn ons that were geometrically possible and possessed consistent temporal and spatial ordering. The data were sent to the streak processor in packets, each packet being defined by a "seed sensor" in either the 12 or 25 micron band and all detector turn ons within a user specified time window that had compatible signal-to-noise ratios. Any streak derived from the packet was constrained to contain the seed sensor. Ordering was confusing because there was spatial overlap in detectors in both the down-range and cross-range directions; because debris crossing times for the most interesting streaks were comparable to or less than the integration times, time confusion had to be considered in the analysis.

At this time, the algorithms have only been tested on isolated sets of data. Setting a 10-second window with a signal-to-noise ratio of 7 in the 12 and 25 micron sensors, one of the test sets of data showed evidence of episodic debris detection. This activity was found to occur over a 20-second interval and the data were summarized in table 3. To determine whether the activity was associated with images crossing the field-of-view or whether the activity reflected randomized noise in the individual detectors, five sets of randomized data were run for comparison. The randomization maintained the same temporal distribution as the actual data. Note that there is considerable redundancy in the counting

of streaks of different lengths, in the sense for example, that a single 4 hit streak implies 3 three-hit streaks, all of which would appear as counts under the 3 hit streak list. Our preliminary conclusion is that the data imply images crossing the focal plane, although the relatively slow rate of crossing and strength of the signals would indicate that most of the images must have come from debris just released from IRAS and drifting through the field-of-view.

TABLE 3.- EPISODIC DATA FROM IRAS COMPARED TO RANDOM NOISE

| | 3 hit streaks | 4 hit streaks | 5 hit streaks | 6 hit streaks |
|---|---|---|---|---|
| Data | 1078 | 494 | 96 | 4 |
| Random sample 1 | 649 | 76 | 0 | 0 |
| Random sample 2 | 828 | 209 | 17 | 0 |
| Random sample 3 | 543 | 73 | 1 | 0 |
| Random sample 4 | 511 | 80 | 11 | 0 |
| Random sample 5 | 749 | 160 | 29 | 0 |
| Random average | 656 | 120 | 12 | 0 |

## MICROPARTICLE DEBRIS STUDIES

### Spacecraft Windows

Since the beginning of the space program, all spacecraft windows from manned spacecraft have been examined for impact pits. Of particular interest were the hypervelocity pits, which were assumed to be caused by micrometeoroids. The only hypervelocity pit found on a Mercury window was slightly less than 1 mm in diameter and some iron was found in this crater, indicating a possible iron micrometeoroid. A 0.1 mm pit was found on a Gemini window, but no residual material was found in the pit. Many craters were seen on the Apollo windows from the 84-day Skylab mission. Both micrometeoritic and man-made debris impacts, the latter indicated by aluminum and paint pigment chemistry in the projectile residuals, were found on these windows.

During the Space Transportation System (STS) program, 13 windows have been swapped out because of pitting. Because these windows are expensive (approximately $50,000), the pits are usually polished out and the window reused. However, a pit found on the STS-7 window was approximately 4 mm in diameter, too large to be polished out. Consequently, this window was investigated for impact with orbital debris. The impact feature was created in a hypervelocity impact with a projectile approximately 200 microns in diameter consisting of $TiO_2$, K, Al, and C, a chemistry indicative of a paint pigment flake. This even provides one of the data points in our characterization of debris flux as a function of size as shown in figure 2. The swap out of this window represents the first time that a spacecraft was repaired because of impact with man-made orbital debris.

Solar Maximum Satellite Returned Surfaces

Approximately 2.4 $m^2$ of material returned by the Solar Maximum satellite servicing mission (STS 41-C) have been completely examined optically for large features. Specific impact features have been examined by electron microscope to get detailed impact morphology and elemental analysis of the impacting particles. The materials consist of thermal control louvers from the attitude control system box (1 $m^2$) and thermal blankets from the attitude control system box and main electronics box. The sizes of impacting particles ranged from submicron to approximately 1 millimeter in size. The features included both holes and craters, and in the thermal insulation material, penetrations through multiple layers of insulation material. Optical scanning was performed on all of the material to identify features of interest[26].

Two large impacts were observed on the thermal blankets. One impact resulted from a projectile of approximately 1 mm diameter having a pure silicon composition. The largest impact on Solar Maximum penetrated all layers of the thermal blanket and created a pit on the aluminum surface. The analysis of the residue indicated the impacting projectile consisted primarily of tungsten and bismuth.

The thermal louver material was found to be more easily analyzed. Sixty-five holes were found in the louvers. Elemental analysis of rim material in 60 of the holes indicated that 7 were a result of impacts with man-made debris and 6 occurred in regions of significant contamination, so that no source could be attributed to the projectile[27]. The size of holes range from 180 to 870 microns. Craters were found in the louvers ranging in size from 0.1 to 270 microns[28]. Sixty of the 600 craters in the size range from 10 to 270 microns were analyzed for projectile chemistry. Across this size range there is a clear shift from predominantly meteoroid impacts at the larger sizes to predominantly man-made debris impacts at the smaller sizes. Of the craters, 33 were categorized as resulting from man-made projectiles and 23 from meteoroids.

Cumulative flux curves have been calculated for both the holes and the craters with the results shown in figure 16. Note that the abscissa values are sizes of the impact feature, and the fluxes are calculated from the number of impacts per unit area of the Solar Maximum surface. The meteoroids will be moving at a higher velocity (approximately 20 km/sec) and will have different density characteristics than man-made debris, so that relating the impact feature to projectile size for comparison is not simple; this scaling is currently being assessed and will be reported at a later date. Paint pigment particles are the most commonly seen man-made debris objects, with aluminates from solid rocket motor exhaust being second most common.

During the initial investigation of the Solar Maximum surfaces, a very large amount of paint contamination was also found. This paint encountered the Solar Maximum surface at low velocity and is thought to be contamination associated with the rendezvous and servicing operations. Besides paint contaminants, some human waste has been found impacting the surface in microparticle form at low velocity. The presence of these contaminants clearly shows that rendezvous and servicing missions to orbiting spacecraft have the potential to degrade the performance of spacecraft being serviced. Besides the low impact velocity contamination, there is evidence of 1 to 2 km/sec impacts on Solar Maximum; the source of this material is unknown.

While the major effort in this project has been to analyze impact features down to 10 microns, which can be attributed to encounters with objects in orbit, some effort is also being made to analyze features below 1 micron, which show large flux values. The interpretation of this data is difficult since some of these features must have arisen from impacts of secondary fragments created by collisions elsewhere on Solar Maximum.

PALAPA Satellite Returned Surfaces

Both solar cell and thermal blanket material from the PALAPA satellite were sent to NASA for examination for orbital debris impacts. Eight solar cells were received, each with a prominent impact feature, along with a single sample of thermal blanket, of which 6432 $cm^2$ were scanned. All of the material showed evidence of handling, and this makes the analysis of the chemistry of the impacting particles difficult.

Eight impacts into the PALAPA solar cells were examined and final data are being processed. A survey of less than 50 micron impacts will be done optically to locate impacts; further SEM inspection is planned.

The PALAPA thermal blanket material was scanned using a Bausch and Lomb stereo zoom microscope at 7X power. The thermal blanket yielded 49 impacts to a limiting size of 70 microns; 43 of these were holes in the first layer and 6 craters. Core samples were taken at all of the impact sites and yielded 95 samples as follows:

a. 6 from the craters
b. 43 from the first layer holes
c. 45 from the underlayers
   (1) 41 second layers
   (2) 2 third layers
   (3) 2 fourth layers
d. 1 from a flaw in the material

The craters were 50, 55, 60, 70, 75, and 90 microns in diameter. The size distribution for the holes was

| Size (microns) | Number of holes |
|---|---|
| 70-100 | 12 |
| 101-150 | 15 |
| 151-200 | 6 |
| 201-250 | 3 |
| 251-300 | 1 |
| 301-350 | 2 |
| 351-400 | 2 |
| >400 | 2 |

The elemental analysis to determine the type of projectiles hitting PALAPA is in progress. Preliminary analysis indicates that contamination associated with the handling of the samples prior to delivery to NASA may be masking the chemical composition of the impacting particles. A large amount of sodium, potassium, and chlorine is associated with all of the impact features, but not with the material itself.

Other Microparticle Laboratory Studies

There have been several projects other than Solar Maximum using the SEM laboratory facilities. To assess materials for orbiting cosmic dust collection, witness plates on STS 61-B were exposed to the exhaust plume of a PAM D2 solid rocket motor (SRM). This work has been reported by Ver Ploeg[29]. Impact speeds were 3 km/sec or less, more typically 2 km/sec or substantially below orbital impact speeds. A variety of materials were used in this experiment, and the resulting flags were examined for particle retention, plastic flow on impact, and surface degradation. Metallic collecting materials displayed cratering with chemical and physical evidence of $Al_2O_3$ particle impacts. Glasses retained almost no trace of the impacting particles and displayed much greater surface degradation than did metals. Typically, glasses showed a front surface spall zone six times the diameter of the central pit.

There is an ongoing program to collect cosmic dust in the stratosphere. The material collected in this program has shown an increasing level of contamination from man-made debris, primarily in the form of aluminum oxide. Computation of the trajectories of these particles, which are all less than 10 microns in diameter and originate from SRM firings, indicate that they will deorbit at very high altitude (approximately 350 km), and will survive deorbit with very little heating[26]. There is, therefore, a fairly rapid communication between the sources of small debris in orbit and airborne collection of that debris in the stratosphere.

Finally, there is a low level program to study spacecraft paints. Although most of the paint found on Solar Maximum was determined to be contamination, the elemental analysis of impact features indicates that paint is also a significant component of the orbiting microparticle ($<300$ micron) population. To understand the processes that might lead to paint being released into the environment, spacecraft paint samples were placed in a plasma etching chamber and the degradation of the paint with time investigated by SEM. The paint, which initially has a very complex structure, experiences a breakdown of the organic binders and develops a morphology very similar to exposed spacecraft paints. As paint ages, binders will erode away and pigment particles will be released into the environment.

Facility for the Optical Inspection of Large Surfaces (FOILS)

The FOILS is used to support research on the type and distribution of orbital debris material and natural micrometeoroids. The small size of the typical impact features being examined and their subsequent geochemical analysis necessitates the requirement for this facility to be a class 10,000 clean room. Satellites and optical parts are optically scanned employing a special Wild microscope mounted on a computer driven Mann comparator. The operator monitors the scanning procedure using a

dedicated television screen. A special coring apparatus is used to detach the more interesting sections from the large scanned surfaces.

SEM Laboratory

A variety of instruments supports the analysis of microparticle impacts found in returned spacecraft surfaces. These include instruments for preparing the samples, imaging and recording morphology in impact features to submicron sizes, performing chemical analysis of impacting particles to distinguish man-made debris from meteoroids, and providing facilities to process and archive the data.

The SEM Laboratory includes

a. JEOL 100cx Analytical Electron Microscope - Capable of operation in SEM (scanning), TEM (transmission), or STEM (scanning transmission) modes. In the TEM mode magnification ranges from 20 to 300,000X, and is primarily used in the analysis of ultrathin sections and small grains (<10um) of cosmic dust. The microscope is equipped with a Princeton Gamma Tech X-ray energy dispersive spectrometer (EDS) which uses a Si (Li) detector and PGT-4000T analyzer.

b. JEOL 35CF Scanning Electron Microscope - SEM magnification ranges from 10 to 100,000X. This scope is equipped with four EDS systems: a Si(Li) window, a Be window, a thin window, and a windowless detector all programmed by a PGT-4000T analyzer.

c. ISI SR-50 Scanning Electron Microscope - SEM magnification ranges from 15 to 150,000X. Imagery uses three types of detectors: secondary electron image, backscatter electron image, and cathode luminescence detector.

d. JOEL 2000FX - This analytical microscope will be installed before years end. It will have TEM, SEM, and STEM capabilities with maximum magnification up to 1,000,000X and an accelerating voltage of 200 kV.

e. Ultramicrotome Thinsectioning - Thinsectioning is used to take very small particles 3 to 15um and cut them into layers approximately 800Å thick. This enables us to eliminate contamination of underlying minerals and increases the resolution of the TEM and STEM modes of electron microscopy.

f. Dark Room - The dark room is used to process all black and white electron micrographs and X-ray diffraction data collected from the microscopes as well as process slides for presentations.

DEVELOPMENT OF DEBRIS MEASUREMENT CAPABILITIES

There are three new instrument development projects. One is a study of space-based debris detection instruments, another is the new CCD debris telescope, a ground-based dedicated debris telescope that has been designed and is now being fabricated, and the third is a ground-based radar capable of observing subcentimeter debris.

## FLIGHT EXPERIMENT - PHASE A FEASIBILITY STUDY

An examination of the data regarding what is known about the on-orbit particle flux as a function of particle size shows that the flux increases as debris size decreases. A collision with a very large object (characteristic dimension on the order of a meter) would be devastating for any spacecraft; however, because of the low flux, the probability of such a collision is low. On the other hand, the collision probability, for the same spacecraft with a very small (submillimeter) object, is quite high; however, because of the small mass associated with such particles, the collision is likely to be abrasive in character (i.e., sandblasting) as opposed to devastating. Our knowledge of large objects in the LEO environment is fairly complete by direct observation. Our knowledge of very small objects at 500 km is fairly good because of recovered spacecraft surfaces. However, there is a range of intermediate sizes at all altitudes and for small sizes above 500 km for which the LEO environmental parameters are poorly known. These present a threat of unknown characteristics to operation in LEO -- the characteristics of the objects themselves and their population characteristics will ultimately be required for design, planning, and safety purposes. For these reasons, in part, an experiment has been proposed to fly an orbital debris detection telescope in the Space Shuttle payload bay in the early 1990's.

The phase A funding for the Shuttle flight experiment (FLTEX) study was provided upon review of a proposal to the Office of Aeronautics and Space Technology (OAST) on the "In-Space Technology Experiments Program." During phase A, a number of technical issues were addressed to verify the feasibility of the proposed experiment. The areas of concern were (1) particle characteristics, detectability, and telescope specification requirements, (2) mission profiles consistent with highest probability of mission success, (3) detector requirements, and (4) anticipated data acquisition rate. Figure 17 is an artist's concept for the instrument in the Shuttle bay. Figure 18 shows two alternative concepts for an all-reflecting Schmidt system being considered as a consequence of the phase A study.

Based on an assessment of the flux data available for very large and very small orbital debris pieces, planning estimates were made for the size range of greatest interest (1 to 30 mm). Using these approximate flux values together with orbital mechanics considerations, the performance requirements for the debris detection system, including approximate telescope diameter and field-of-view, were assessed.

In addition to a telescope system that is capable of obtaining data under good conditions, it was necessary to determine under what circumstances of mission profile suitable conditions could be obtained. From this portion of the phase A study it was found that high inclination, high altitude orbits produced the longest duration of favorable observing circumstances; that is, the particles to be detected were located opposite in the sky from the sun (phase near 0°) and observable throughout each revolution.

The experiment will be designed to obtain simultaneous optical and infrared observations for gathering information about the particle physical characteristics (e.g., albedo) as well as their numbers. The phase A effort strongly indicated the use of a large (2048-by 2048-bit) optical CCD ringed by infrared detectors for observations in both wavelength regions as any given particle crosses the focal plane. The focal plane will be chilled to liquid nitrogen temperatures to reduce background noise and enhance signal detectability.

Because of the large size of the detector area and a readout rate that will need to be at least 10 frames per second, the high data rate of digital data implied precludes direct downlink; rather, an onboard tape recorder capable of recording digital data at approximately 100 Mbps will be used. For function verification a video pick-off may be used and display made possible on the aft flight deck.

The phase B study has been approved by OAST to begin in CY89, and will further define the requirements for the development and flight of the orbital debris telescope.

## A PORTABLE CCD DEBRIS TELESCOPE

During the 2 years prior to this reporting period, an ongoing observational program, at visible wavelengths, demonstrated the usefulness of a small, portable telescope in the gathering of data on orbital debris. The primary instrument during this early phase of the program was an 8-inch in diameter LENZAR telescope coupled to a light-intensified camera system and video recorder. This telescope and detector combination was employed in several field campaigns to New Zealand and the state of Washington.

The LENZAR experience demonstrated not only the usefulness of the small, portable orbital debris telescope, but also served as a motivator for the development of a second generation orbital debris telescope, optimized for debris work and a state-of-the-art detector such as a CCD at the focal plane. To achieve the construction of such a system, several subcontracts were let for (1) optical design, (2) CCD detector fabrication, and (3) telescope optical/mechanical construction.

A design study was initiated with Spectrometrics, Inc., of Tucson, Arizona, regarding the basic optical characteristics of the telescope. The set of possible designs was constrained by NASA requirements for such parameters as field-of-view, image quality requirements, etc. The subcontractor supplied two basic design types: (1) a classical Schmidt and (2) a Maksutov. The Schmidt design was chosen. Several variations of the Schmidt design were considered and one submitted to the optical/mechanical contractor for telescope fabrication.

The contract for the construction of the optical and mechanical components of the orbital debris telescope was awarded to Optomechanics Research, Inc., of Vail, Arizona. This subcontractor is responsible for (1) the grinding of all optical surfaces to the design specifications, (2) the construction of the mechanical telescope assembly in which the optical system will reside, and (3) the interfacing of the optical/mechanical system with the CCD detector subsystem (supplied by another subcontractor). These tasks have been completed and the integrated performance of the telescope/detector system have been tested by NASA/Lockheed. The telescope is shown in figure 19.

The detector for the new ground-based telescope is a thermoelectrically-cooled CCD camera system supplied by Photometrics, Inc., of Tucson, Arizona. This highly sensitive state-of-the-art detector will allow for the acquisition of digital images. A portable command, control, and acquisition hardware and software system, a Photometrics DIPS 184, is being used for data acquisition in the field.

The entire system should be ready for delivery in early to middle CY89.

## DEBRIS ENVIRONMENT CHARACTERIZATION RADAR (DECR)

The most useful data acquired for orbital debris analysis have usually been radar data acquired by radar systems designed for other purposes. Therefore, it seemed apparent that a specially designed, dedicated debris radar would be a very useful development. A summary of the requirements for a dedicated ground-based radar to detect debris in orbit is presented in table 4. This radar, called the DECR, is scheduled to begin operation in 1992, so that the results of the data acquisition can be factored into Space Station operations and design decisions. Rather than trying to acquire orbital element data, the DECR will be used primarily to establish a statistical picture of the small debris in orbit to 1000 kilometers altitude. A radar similar to the proposed DECR is shown in figure 20.

A suitable version of this radar could be built inexpensively with commercially available hardware. A summary of the JSC baseline system is provided in table 5. Procurement of the radar for NASA is being handled by the Jet Propulsion Laboratory. A request for proposals has been released.

## SMART CATALOG PROGRAM

A cooperative effort between NASA and the Air Force Space Command (AFSPACECOM) was started to explore how best to satisfy the requirements for monitoring the orbital debris environment with the requirements imposed by the AFSPACECOM charter to monitor the space environment for hostile objects. In fact, when there are extensive military assets in orbit, hostile objects could appear as debris. This first study was conducted by Teledyne-Brown Engineering in Colorado Springs, Colorado, and assessed both data acquisition requirements and data processing and interpretation requirements[30]. The study was completed at the end of CY88, and recommends the concept of a hybrid database, consisting of both tracked object data and statistical sampling of the environment. This concept is logically very similar to the evolution modeling concepts of the EVOLVE program, and further development of that program will demonstrate the effectiveness of this hybrid database approach.

# SHIELDING AND VULNERABILITY RESEARCH

## HYPERVELOCITY IMPACT MODELING

The orbital debris program sponsors an ongoing effort to develop theoretical models sophisticated enough to supplement and extend knowledge attained through experimental programs. The driver for this effort is, of course, the fact that experimental programs are not able to match the projectile size or impact speeds experienced in collisions between orbiting objects. Moreover, experimental shots are sufficiently expensive that even parameters that are attainable, such as impact angle, may not be spanned with sufficient experimental data. The modeling program is made difficult, however, because new experimental data from previously untested conditions tend to correct rather than to confirm previous theoretical results.

TABLE 4.- CRITICAL REQUIREMENTS FOR GROUND-BASED DEBRIS RADAR (NEEDED TO SUPPORT SPACE STATION DESIGN)

| Characteristic | Requirement | Rationale |
|---|---|---|
| Debris size and altitude | 1 cm diameter (RCS = 0.785 cm) at 500 km | Shielding design for habitability areas |
| Probability of detection at required size/altitude | 50 percent | Confidence in data |
| False alarm rate | 1/10 of event rate | Confidence in data |
| Scintillation characteristic | Swerling 1 | Irregular object, "worst case" |
| Detection rate at required size/altitude | 1 event/day | Achieve statistically significant results in an acceptable time (beam with >0.25°) |
| Altitude range | 300 to 600 km | Space Station operation altitude |
| Altitude | +or- 25 km | Confidence in flux at given altitude |
| Inclination | None | Currently not required for shielding |
| Eccentricity | None | Accept whatever data can be derived or obtained |
| Inclination coverage | All inclinations greater than 26.5° | Cover more than 90 percent of debris sources |
| Schedule | Radar operating August 1991 | Support Space Station pressurized volume critical design review (CDR) |

TABLE 5.- BASELINE RADAR PRIMARY CHARACTERISTICS

| Characteristic | Value |
|---|---|
| Peak power | 200 KW |
| Carrier frequency | 8.56 GHz (= 3.5 cm) |
| Pulse repetition frequency | 100 Hz |
| Pulse width | 2000 μ sec |
| Field-of-view | 0.25° (9 m antenna) |
| Pointable | |

In consequence, one of the primary modeling efforts has been to assimilate existing experimental programs and to suggest new experimental programs that will support an empirical scaling modeling effort; that is, to use existing data to extrapolate to conditions that have not been previously tested. This work has been lead by Cour-Palais and co-workers[28,29]. The objective in this activity has been to establish scaling laws for projectile velocity and mass and projectile to shield density ratio in multi-layered shields. This modeling approach has proven successful in the past and offers a mechanism for theoretical modeling involving complex materials, where there may be no simple equation of state.

For some more simple materials, a program of hydrodynamical modeling has been started. The AUTODYNE program, a personal computer (PC) derivative of the PISCES code, is being used to study projectile interactions with nonmetallic thin shields. At this time the Lagrangian code is not being worked because the high impact speeds require frequent rezoning and loss of definition of the materials involved. Modification of the code to include an Eulerian processor should improve its operation.

The University of Texas at Austin is similarly involved in a modeling project primarily directed towards understanding the fragmentation of the projectile on impact[33]. Both spherical and flat disc projectiles impacting thin aluminum shields have been modeled. A preliminary conclusion of the effort is that the projectile may be viewed as exploding upon impact, so that parts of the projectile may be accelerated in the forward direction as the impact is occurring.

## HYPERVELOCITY IMPACT STUDIES

JSC has an extremely active experimental hypervelocity impact research program. The primary objectives of the program have been to study new materials and new designs for spacecraft shielding, to provide an experimental database for the modeling project work, to identify and develop new research areas, and to provide testing support for assessment of hypervelocity impact on subsystems and components of large programs such as Space Station.

New types of materials have been investigated for use in shielding and debris collector concepts. In both cases, materials and designs are needed that can undergo hypervelocity impact, slow down or stop the impacting object while producing a minimal amount of secondary debris released to the environment, and impose minimal weight penalties. In one project, promising foam materials that could

reduce the velocity of a debris particle by 2 percent were tested and found to produce very little fragmentation in the projectile. A long-term testing program on nonmetallic bumper materials has also been conducted[36,37,38]. A study was conducted on the potential hazards to spacecraft from secondary particles produced by hypervelocity impact[39].

Tests have been run on two of the space suit designs currently being considered for Space Station and on truss structures being considered for Space Station[40]. In testing the space suits it was determined that the planned number of hours of extravehicular activity (EVA) was inconsistent with the level of reliability being demanded for the habitability areas in the Space Station. In addressing the options of reduced EVA, harder space suits, or lower reliability, NASA is now baselining the use of more resistant space suits.

A recent shooting program into pressurized vessels has provided new insight into possible causes of breakups of stages in orbits[41]. With only modest internal pressures, the propagation of damage from debris impact can lead to catastrophic destruction of the vessel, with an attendant significant anomalous propulsive thrust and pressure wave propagation through the structure, for much smaller debris sizes than would affect an unpressurized vessel in the same way. Consequently, collisions with much smaller debris could cause a catastrophic destruction of a structure such as the ARIANE V16; such a collision would be more probable than was previously thought. This work also has important implications for Space Station, which is planning to have high pressure tankage and transmission lines on the structure.

Finally, a hypervelocity launcher development project, which fires a shaped charge cutoff to make a cylindrical intact particle with a length-to-diameter ratio of 3, is being supported. This development effort is being driven by the current velocity limit of 7 to 8 km/sec of light gas guns, a velocity significantly below the expected impact speed in orbit of 11 km/sec. The shaped charge launcher will be able to accelerate 2-gm projectiles to 12 km/sec when it is fully developed.

## HYPERVELOCITY IMPACT RESEARCH LABORATORY (HIRL)

The HIRL at JSC is used to pursue an active research and operations support program of hypervelocity impact testing. This laboratory supports the Space Station through many tests, simulations, and analyses of hypervelocity impact damage to materials and components such as the EVA space suits and truss structures. These studies provide inputs to the design and shielding requirements for all spacecraft and components exposed to the debris environment. Scale models of spacecraft and both pressurized and unpressurized upper stage fuel tanks have been studied to better understand the consequences of impacts between these objects and relatively large debris objects in orbit. In addition, the laboratory supports the testing of advanced, lightweight materials and new shielding concepts to provide improved shielding and less secondary debris generation for future space systems. In most cases, the material characteristics and encounter geometries are sufficiently complex that the most effective research tool available is the HIRL, with theoretical modeling an activity that must rely on a database and empirical models derived from test data.

During the past year the HIRL was given a building of its own to adequately house a more active shooting program with a larger gun. Currently two small guns are housed in the building; the larger

gun can fire 4.3 mm projectiles to speeds > 7 km/sec, and the smaller 1.7 mm projectiles to speeds of 9 km/sec. In the next year, a larger gun is being brought from Ames Research Center which will fire 1.27 cm (1/2 inch) projectiles to speeds of 7 km/sec. The small guns are capable of firing very small (approximately 100 micron) projectiles using a sabot and can be used to provide laboratory calibration of the larger impact features as seen on surfaces such as Solar Maximum. The support equipment in the HIRL includes an ultra-high speed rotating mirror framing laser and a shadowgraph camera supporting 20 nanosecond exposure times for up to 80 frames of 35 mm infrared film at 2 million frames per second.

Notable test programs over the past year have included

a. A general advanced shielding and materials research project, leading to a patent disclosure for a new lightweight, nonmetallic shielding concept

b. EVA space suit layups and helmet studies

c. Graphite-epoxy truss studies

d. Propellant tank studies. These have included scale model firings at JSC and full scale testing of pressurized tanks at the White Sands Test Facility in June 1988.

e. Cosmic dust collector concept studies. This project included tests using beryllium projectiles at the White Sands Test Facility in June 1988.

f. Fiber mast support structure for solar arrays (performed for Lewis Research Center)

g. Tests of foam and thin sheet materials for debris sweeper feasibility assessment

In the next year a still more active test program is planned. At this time there are plans for

a. Microsheet concentrator studies to support solar array assessments (to be performed for Lewis Research Center)

b. Studies of Space Station utility trays (housing wires and high pressure fluid lines) and truss nodes

c. Scale model testing of spacecraft and spacecraft subsystems

d. Combined testing of coated plastics with exposure in oxygen plasma chamber to understand material effect of exposure to atomic oxygen in orbit

e. Studies of impact flash

f. Bringing online a new gun capable of firing a 7.3 kg projectile at 1 km/sec. This gun will be used to study low-velocity impact processes for debris up to several centimeters in diameter.

## REFERENCES


1. Kessler, D.J.: Orbital Debris Environment for Space Station. JSC 20001, 1984.

2. Zook, H.A., Flaherty, R.E., and Kessler, D.J.: Meteoroid Impacts on the Gemini Windows. Planetary and Space Sciences, vol. 18, 1970, pp. 953-964.

3. Kessler, D.J., Reynolds, R.C., and Anz-Meador, P.D.: Orbital Debris Environment for Spacecraft Designed to Operate in Low Earth Orbit. NASA TM 100 471, 1988.

4. Reynolds, R.C., Fischer, N.H., and Edgecombe, D.S.: A Model for the Evolution of the On-Orbit Man-Made Debris Environment. Proceedings of the NASA/JSC Orbital Debris Workshop, NASA Conference Publication 2360. 1982, pp. 102-132.

5. Su, S.-Y.: Contribution of Explosion and Future Collision Fragments to the Orbital Debris Environment. Advances in Space Research, 5, 2, 25, 1985.

6. Chobotov, V.A., Spencer, D.B., Schmitt, D.L., Gupta, R.P., Hopkins, R.G., and Knapp, D.T.: Dynamics of Debris Motion and the Collision Hazard to Spacecraft Resulting from an Orbital Breakup. Aerospace Corporation Report SD-TR-88-96, 1988.

7. Su, S.-Y.: On the Velocity Distribution of Collisional Fragments in the New Ejecta Model and its Effect on the Future Space Environment. LEMSCO Report, 1985.

8. Bess, T.D.: Mass Distribution of Orbiting Man-Made Space Debris. NASA Report L-10477, December 1975.

9. Badhwar, G.D., Potter, A.E., Anz-Meador, P.D., and Reynolds, R.C.: Characteristics of Satellite Breakups from Radar Cross-Section and Plane Change Angle. Journal of Spacecraft and Rockets, in press.

10. Badhwar, G.D. and Anz-Meador, P.D.: Determination of the Area and Mass Distribution of Orbital Debris Fragments. Paper presented at the 39th International Astronautical Federation Congress (Bangalore, India), 1988.

11. Kessler, D.J. and Cour-Palais, B.G.: Collision Frequency of Artificial Satellites: The Creation of a Debris Belt. Journal of Geophysical Research, vol. 83, 1978, pp. 2637-2646.

12. Johnson, N.L. and Nauer, D.J.: History of On-Orbit Satellite Fragmentations 3/E. Teledyne-Brown Engineering Report TR CS88-LKD-001, October 1987.

13. Mueller, A.C.: The Decay of the Low Earth Satellite. LEMSCO Report 17250, 1981.

14. Glover, R.A.: Characterization of Satellite Breakup Debris. Final Report to Lockheed Engineering and Sciences Company, December, 1988.

15. Kaya, D. and France, R.: Stand-Alone Element Set Conversion. Final Report to Lockheed Engineering and Sciences Company, October, 1988.

16. Grissom, W., Guy, R., and Olmstead, S.: SATRAK Operator's Guide. TBE Report CS89-LKD-004, Final Report to Lockheed Engineering and Sciences Company, 1989.

17. Talent, D.L. and Petro, A.J.: Removal of Space Debris. Paper presented at the JSC Upper Stage Breakup Conference, May 1987.

18. Tidman, D.A., Thio, Y.C., and Goldstein, S.A.: Removal of Debris from Earth Orbit Using a Ground-Based High Velocity Electrothermal (HVET) Gun. Final Report to Lockheed Engineering and Management Services Company, November 1987.

19. Potter, A.E., Henize, K., and Talent, D.L.: Albedo Estimates for Debris from Various Satellite Breakups. Paper presented at the JSC Upper Stage Breakup Conference, May 1987.

20. Taff, L.G. and Jonuskis, D.M.: Results and Analysis of a Telescopic Survey of Low Altitude Orbital Debris. Advances in Space Research, 6, 7, 131, 1986.

21. Lebofsky, L.L. and Vilas, F.: Thermal Models Applicable for Visual and Infrared Studies of Orbital Debris. Paper presented at COSPAR XVII, 1988.

22. Kessler, D.J.: NORAD'S PARCS Small Satellite Tests (1976 and 1978). Proceedings of the Orbital Debris Workshop, NASA Conference Publication 2630, 1987, pp. 39-44.

23. Jost, R.J. and Noble, S.T.: VHF Radar Backscatter Observations During Delta-180. Systems Planning Corporation. Report 017027, 1987.

24. Jost, R.J.: Reentering Spacecraft Ionization Observations. Systems Planning Corporation. Report 069078, 1988.

25. Anz-Meador, P.D., Oro, D.M., Kessler, D.J., and Pitts, D.E.: Analysis of IRAS Data for Orbital Debris. Advances in Space Research, 6, 7, 139, 1986.

26. Warren, J.H. Zook and Allton, J.: Optical Observations of Impact Features on Solar Max Thermal Blankets and Louvers. Paper presented at Lunar and Planetary Science Conference XIX, 1988.

27. Barrett, R.A., Bernhard, R.P., and McKay, D.S.: Impact Holes and Impact Flux on Solar Max Louver Material. Paper presented at Lunar and Planetary Science Conference XIX, 1988.

28. Bernhard, R.P. and McKay, D.S.: Micrometer-Sized Impact Craters on the Solar Maximum Satellite: The Hazards of Secondary Ejecta. Paper presented at Lunar and Planetary Science Conference XIX, 1988.

29. Verploeg, K.L. and McKay, D.S.: Impacts on Shuttle Orbiter Caused by Firing of PAM-D2 Solid Rocket: Results of STS 61-B Plume Witness Plate Experiment. LEMSCO/NASA Internal Draft Report, 1987.

30. Nauer, D.J.: Smart Catalog Hybrid Database Demonstration Software Operator's Guide. TBE Report CS88-LKD-012 to Lockheed Engineering and Sciences Company, 1988.

31. Cour-Palais, B.G.: Space Vehicle Meteoroid Shielding Design. Proceedings of the 1979 International Workshop sponsored by the European Space Agency, ESA SP-153, 1979.

32. Cour-Palais, B.G.: Hypervelocity Impact in Metals, Glass, and Composites. International Journal of Impact Engineering, vol. 5, no. 1-4, 1986, pp. 221-237.

33. Yew, C.H. and Kendrick, R.B.: A Study of Damage in Composite Panels Produced by Hypervelocity Impact. International Journal of Impact Engineering, vol. 5, 1987, pp. 729-739.

34. Yew, C.H. and Weng, X.: Hypervelocity Impact of Two Spheres. To be published in September 1989 Issue of International Journal of Impact Engineering.

35. Yew, C.H. and Wu, Y.J.: On Modeling of Debris Clouds. University of Texas at Austin, 1989.

36. Yew, C.H., Wang, C.Y., and Crews, J.L.: A Phenominological Study of the Effect of Hypervelocity Impacts on Graphite-Epoxy Plates, 1986.

37. Christiansen, E.L.: Evaluation of Space Station Meteoroid/Debris Shielding Materials. NASA Contract NAS9-15800, Lockheed Subcontract PO 02-001-12718, Eagle Engineering, Inc. Report 87-163, 1987.

38. Crews, J.L. and Stump, W.R.: Preliminary Comparison of Aluminum and Composite Habitation Module Walls and Bumpers Subjected to Hypervelocity Impact. NASA/Eagle Engineering, Inc. Report, 1983.

39. Stump, W.R. and Christiansen, E.L.: Secondary Impact Hazard Assessment. NASA Contract T-256M, Eagle Engineering, Inc. Report 86-128, 1986.

40. Christiansen, E.L.: Investigation of Hypervelocity Impact Damage to Space Station Truss Tubes. NASA Contract NAS9-17900, Lockheed Subcontract PO 02-001-12133, Eagle Engineering, Inc. Report 88-176, 1988.

41. Cour-Palais, B.G. and Crews, J.L.: Hypervelocity Impact and Upper Stage Breakups. Paper presented at the JSC Upper Stage Breakup Conference, May 1987.

## ORBITAL DEBRIS PROJECT STRUCTURE

NASA MANAGER: A. POTTER
NASA DEPUTY MANAGER: J. STANLEY
NASA CHIEF SCIENTIST: D. KESSLER

LESC MANAGER: R. REYNOLDS

### MODELING

- DEBRIS POPULATION
- HYPERVELOCITY IMPACT
- VULNERABILITY

NASA:
- D. KESSLER
- G. BADHWAR
- B. COUR-PALAIS
- E. CHRISTIANSEN

LEMSCO:
- R. REYNOLDS
- P. ANZ-MEADOR

SUBCONTRACTORS:
- GENERAL RESEARCH CORP.
- TELEDYNE BROWN ENGR.
- EAGLE ENGINEERING
- ASTRONAUTICS CORP. OF AMERICA
- UNIVERSITY OF TEXAS
- LARGE SCALE PROGRAMS INSTITUTE

### DATA ACQUISITION

- OPTICAL/IR
- RADAR
- MICROPARTICLE
- SHIELDING

NASA:
- J. STANLEY
- A. POTTER
- K. HENIZE
- J. CREWS
- D. McKAY

LEMSCO:
- R. RAST
- D. TALENT
- R. BERNHARD

SUBCONTRACTORS:
- GENERAL RESEARCH CORP.
- TELEDYNE BROWN ENGR.
- UNIVERSITY OF ARIZONA

### INSTRUMENT DEVELOPMENT

- FLIGHT EXPERIMENTS
- GROUND-BASED RADAR
- GROUND-BASED OPTICAL
- HYPERVELOCITY ACCELERATOR

NASA:
- F. VILAS
- E. STANSBERY
- H. ZOOK
- B. COUR-PALAIS
- K. HENIZE

LEMSCO:
- D. TALENT
- R. RAST

SUBCONTRACTORS:
- SYSTEMS PLANNING CORP.
- OPTOMECHANICS, INC.
- SOUTHWEST RESEARCH INST.
- PHOTOMETRICS, LTD.

### LABORATORIES

- IMAGE PROCESSING (D. PITTS)
- ELECTRON MICROSCOPY (D. McKAY)
- HYPERVELOCITY IMPACT (J. CREWS)
- OPTICAL (F. VILAS/K. HENIZE)
- RADAR (G. STANSBERY)

Figure 1.- Orbital Debris Project organization.

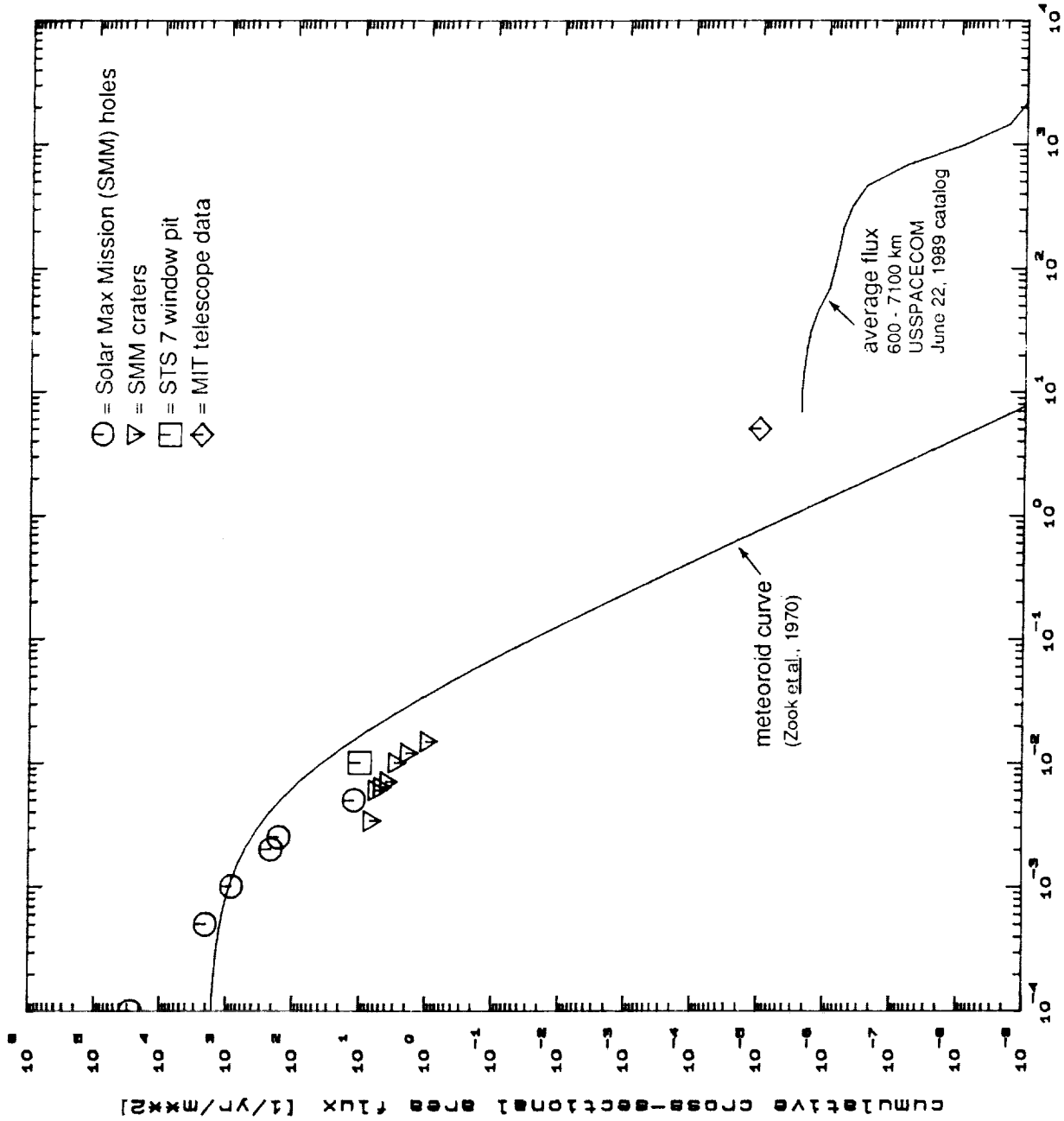


Figure 2.- Current flux[2] compared to existing orbital debris measurements.

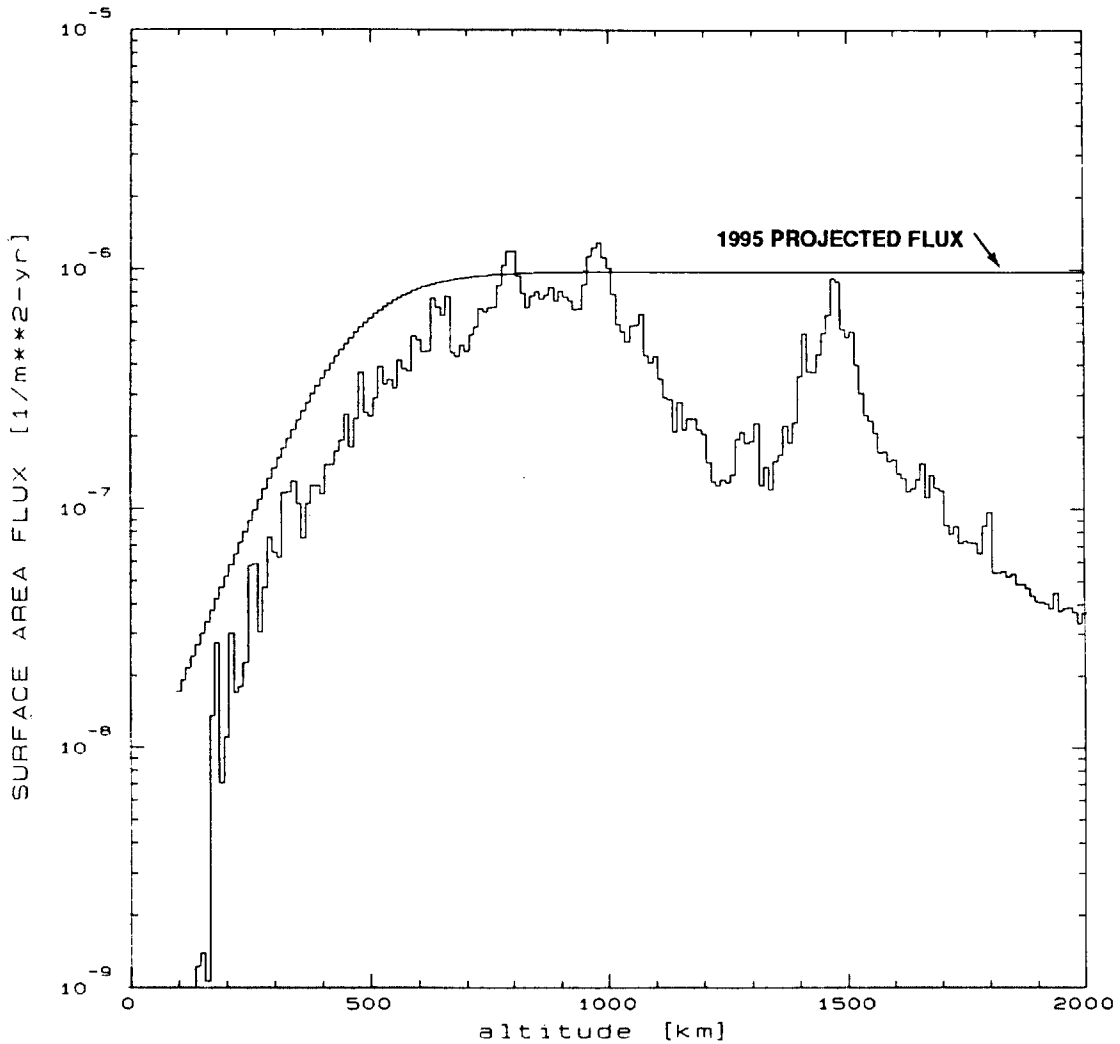


Figure 3.- Debris flux versus altitude for 1995 compared to January 1989 catalogued environment[3].

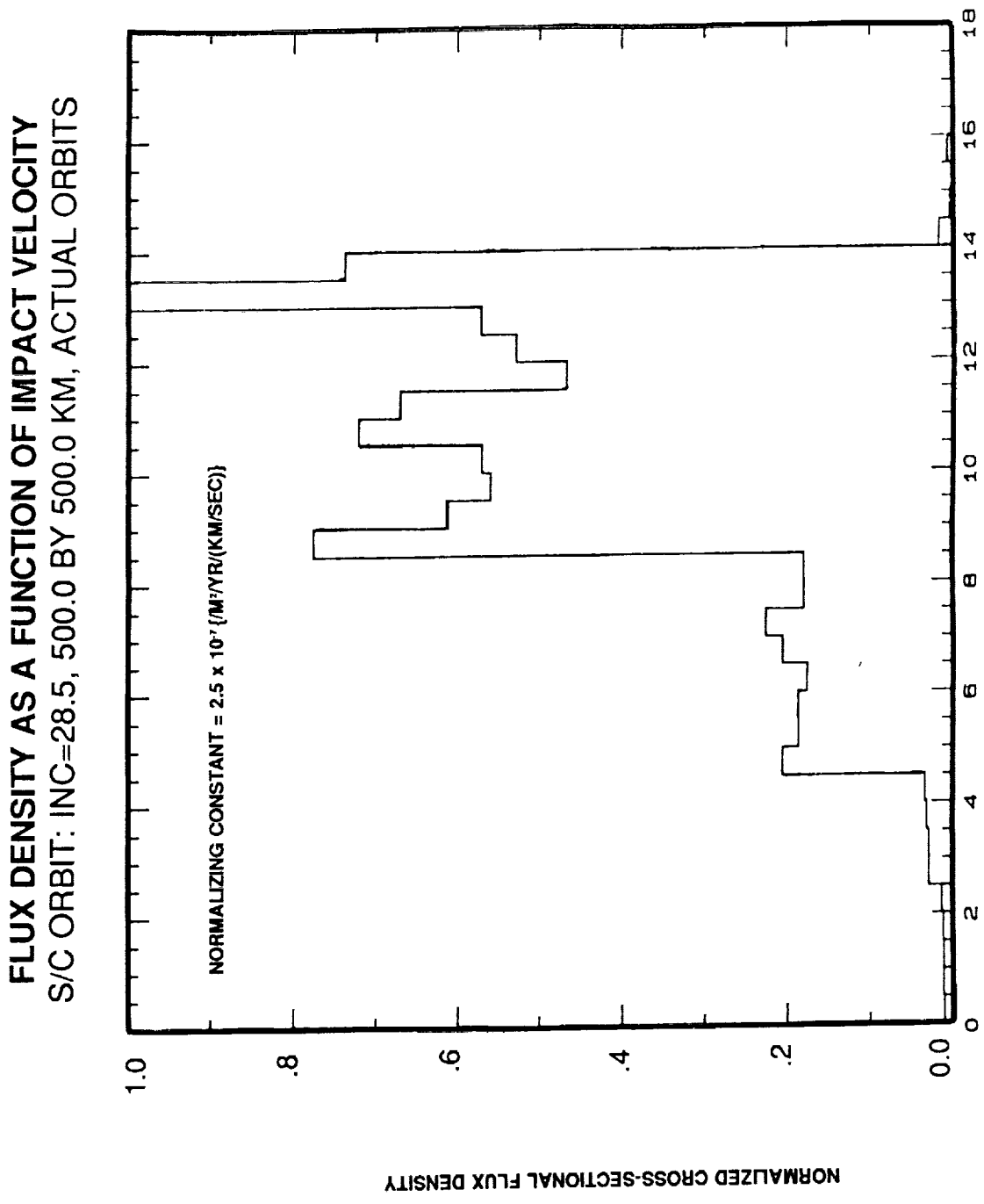


Figure 4.- Distribution in relative impact velocity for a spacecraft in 28-1/2°, 500 km orbit.

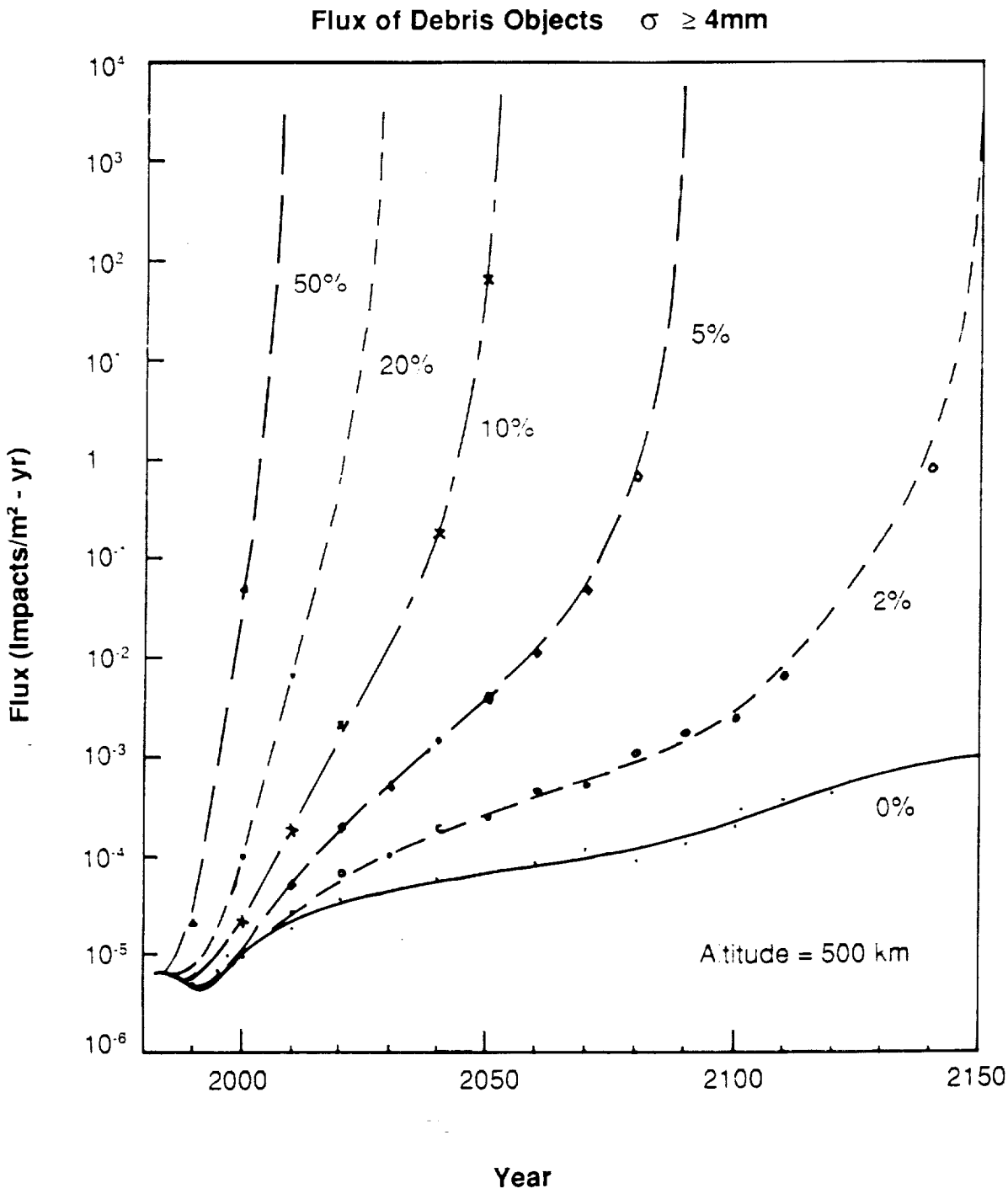


Figure 5.- Debris flux from objects with diameter 4 mm or greater at 500 km altitude with different increases in rate of yearly traffic input.

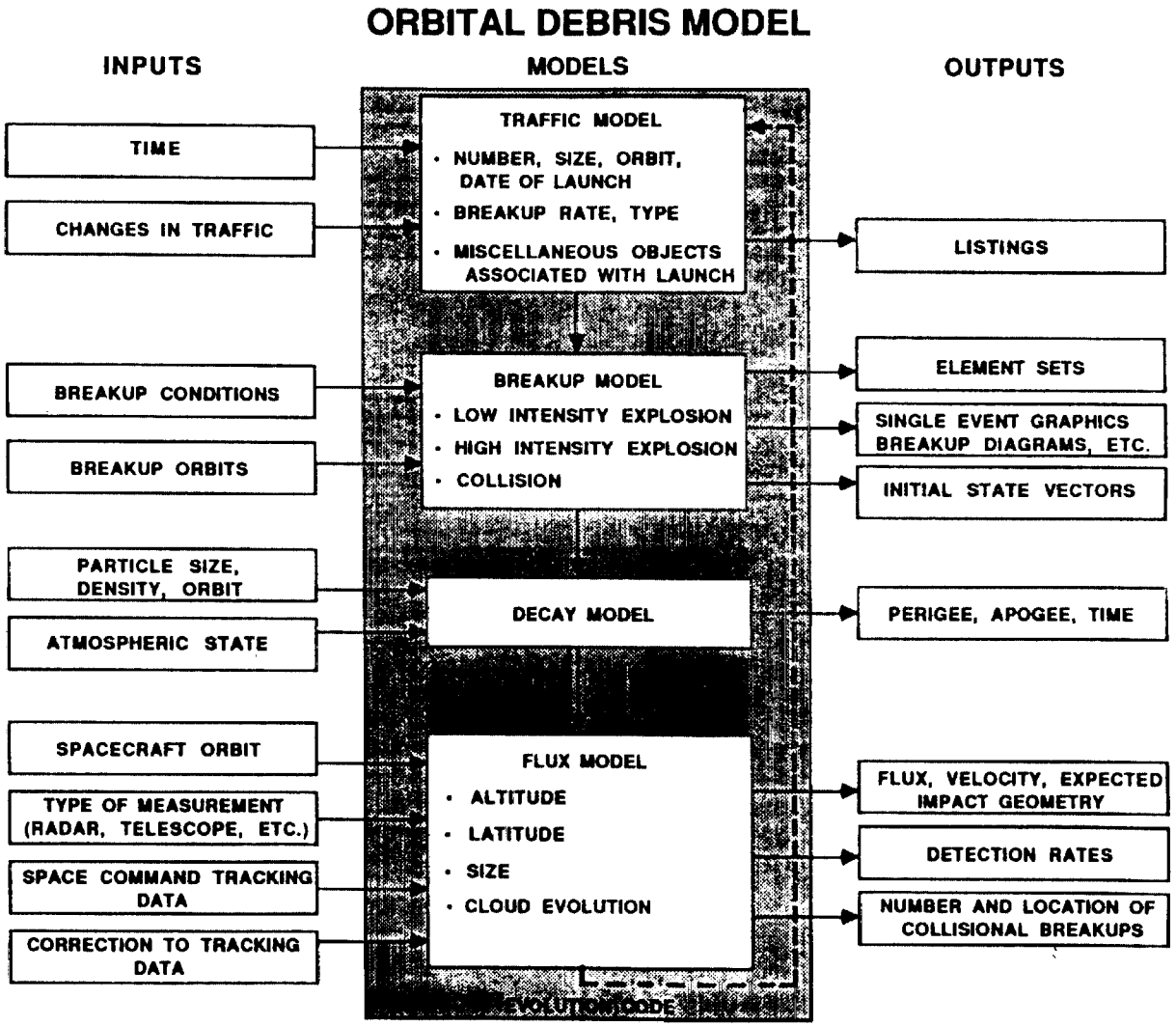


Figure 6.- Logic structure in PROGRAM EVOLVE.

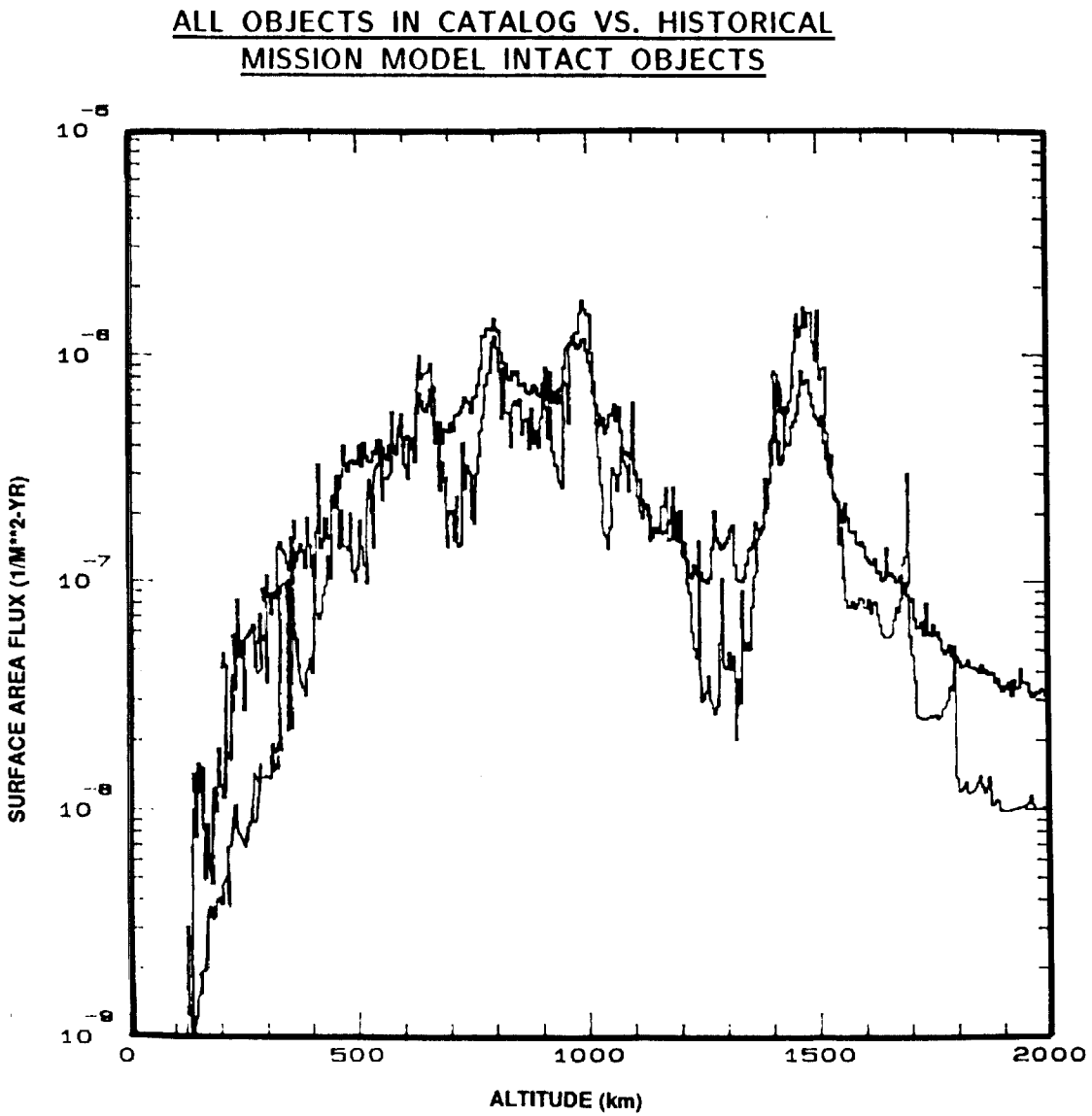


Figure 7.- Flux versus altitude for the current tracked population (top plot) and for intact objects (lower plot) from PROGRAM EVOLVE.

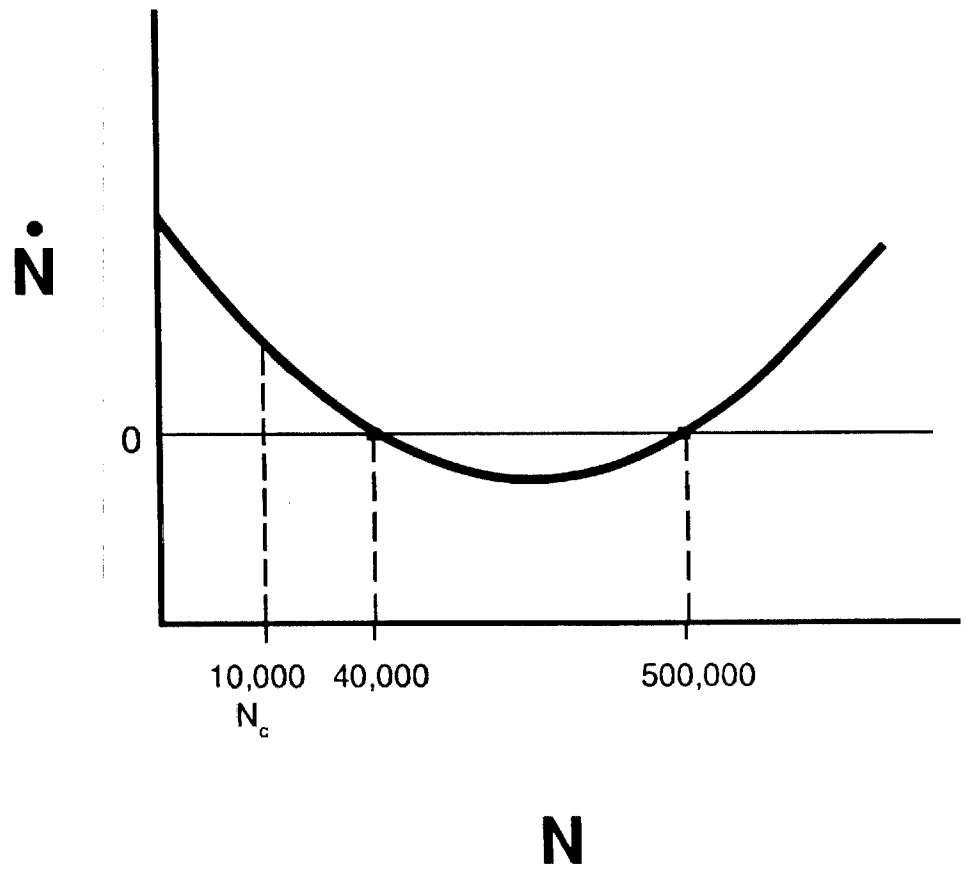


Figure 8.- Debris population growth rate versus population size for best estimate values of A, B, and C for the current population.

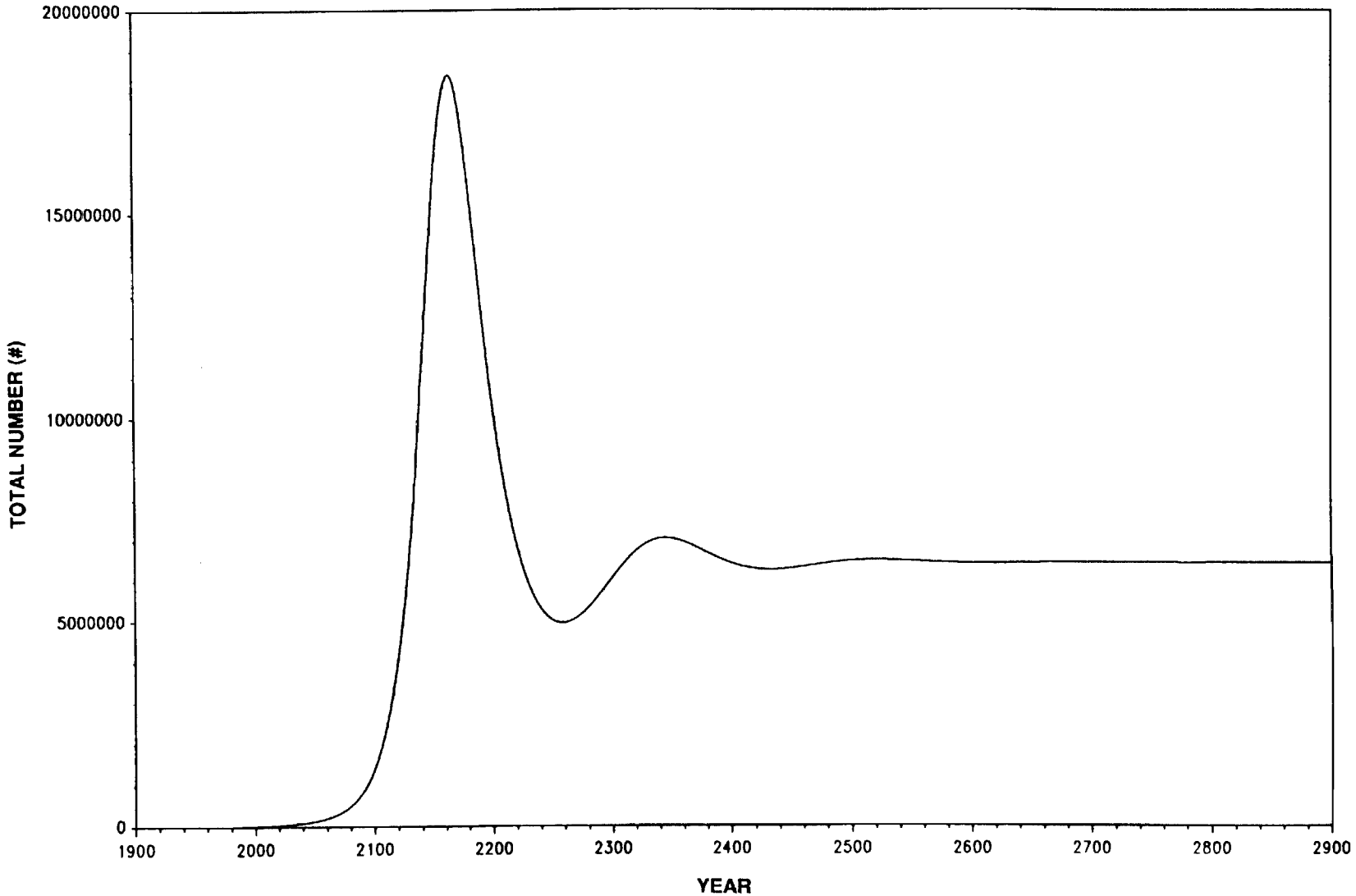


Figure 9.- Population growth using a simple particle-in-box model for 2 percent growth in launch rate through 2020, constant launch rate thereafter.

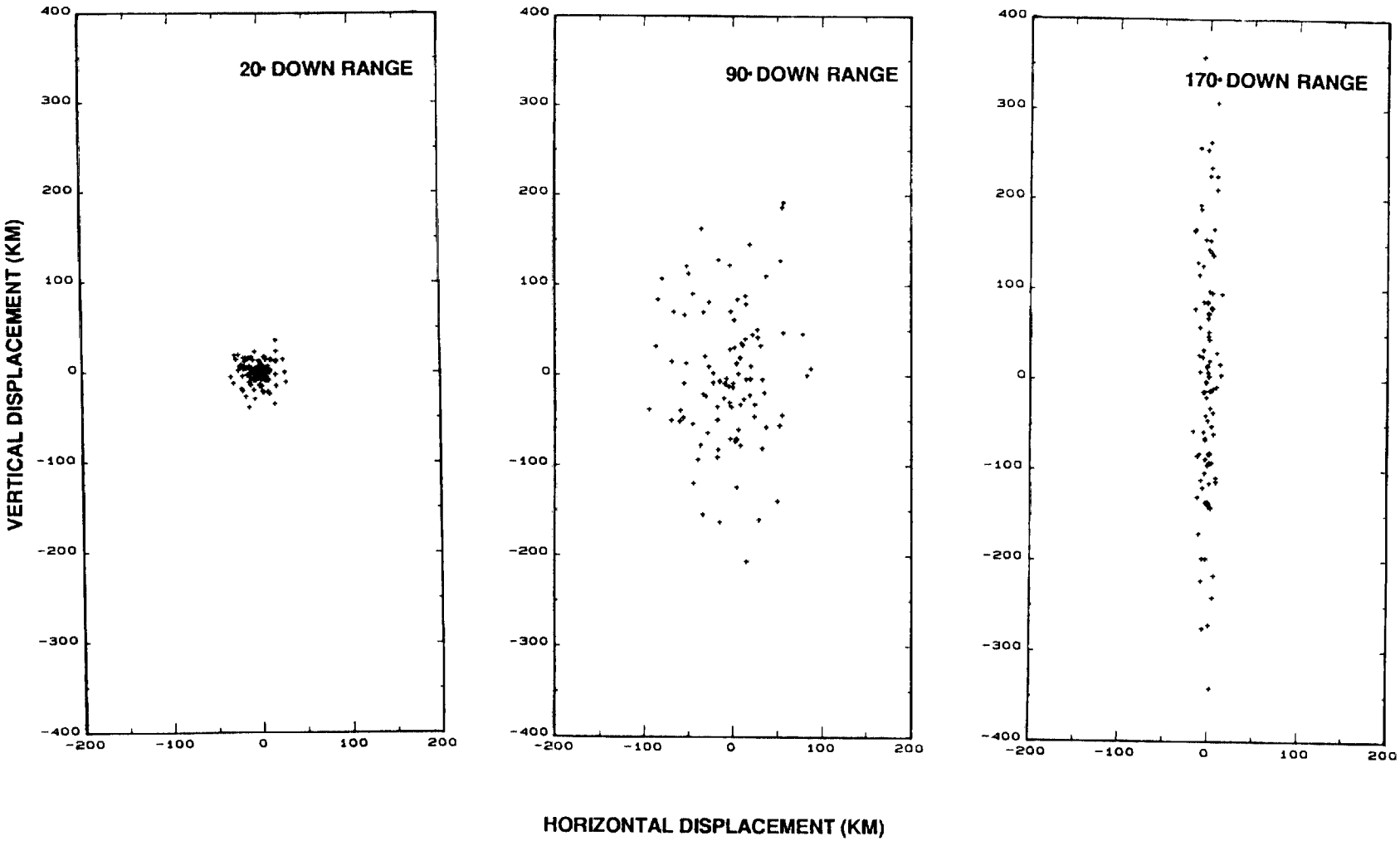


Figure 10.- The penetration pattern for the 100 largest objects in a standard breakup through planes 20°, 90 °, and 170° downrange from the breakup point.

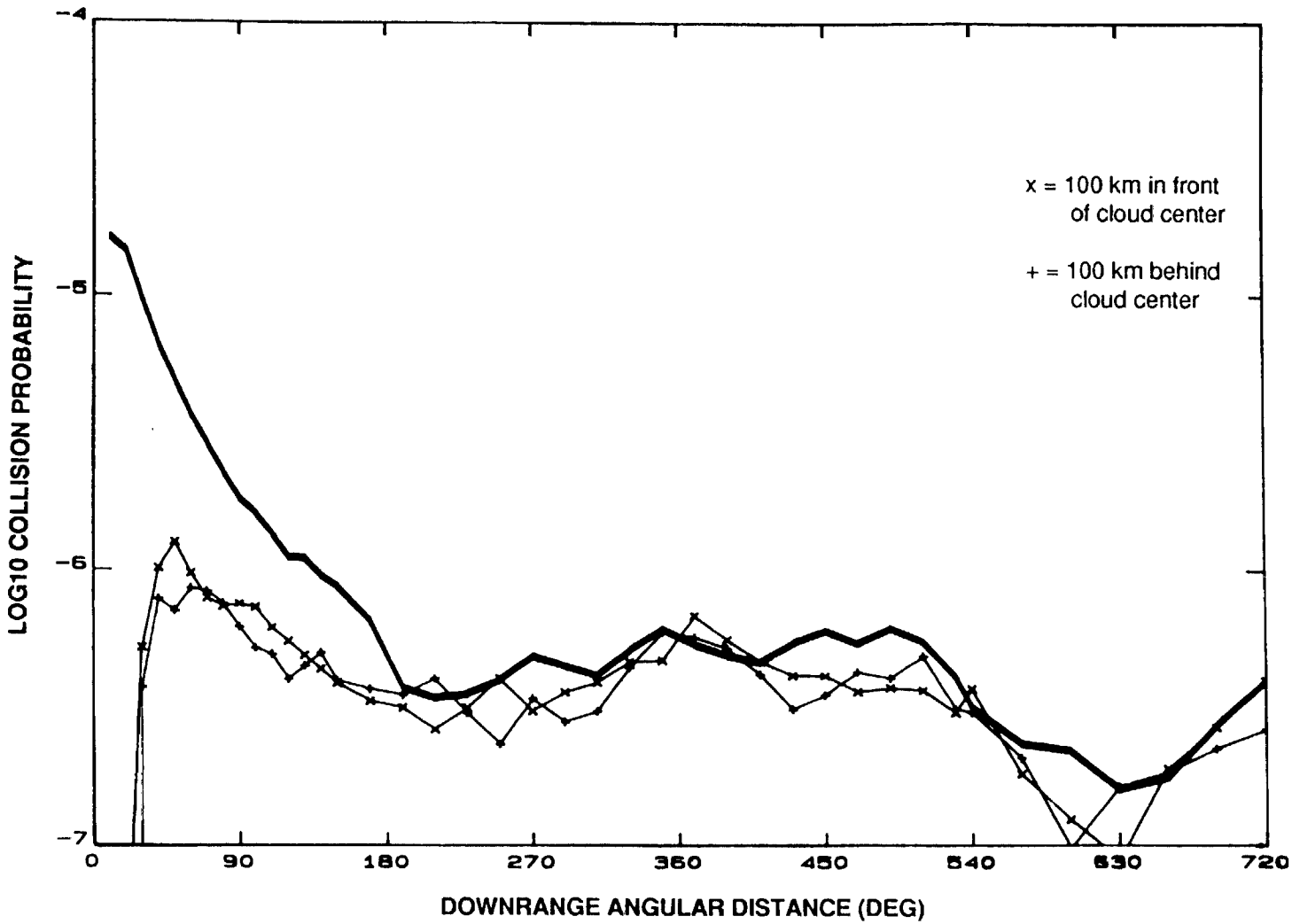


Figure 11.- Collision probability for a 250 $m^2$ spacecraft passing through the center of a debris cloud as a function of distance downrange of the breakup.

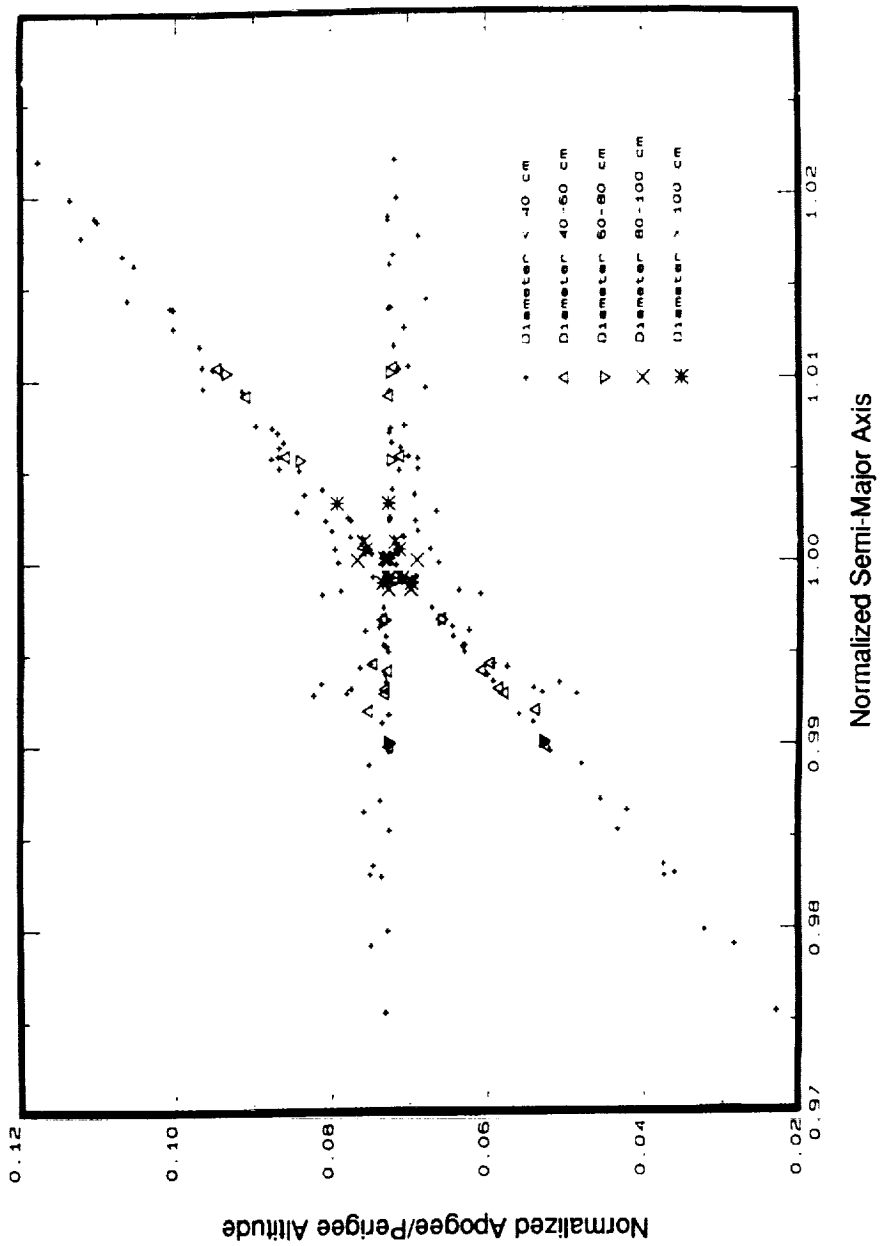


Figure 12.- Breakup plot for the baseline breakup model.

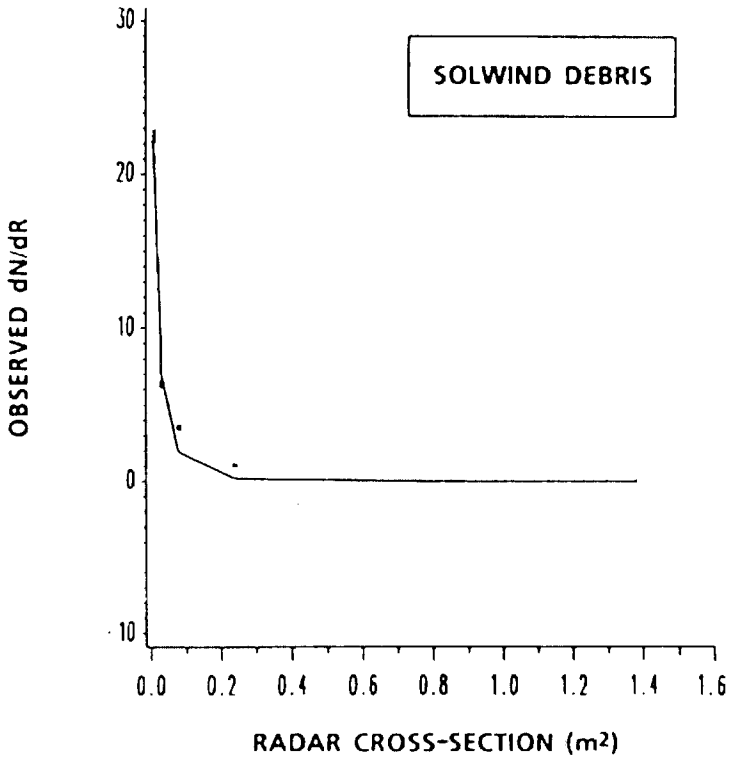


Figure 13.- Fragment number distribution versus size for the SOLWIND breakup.

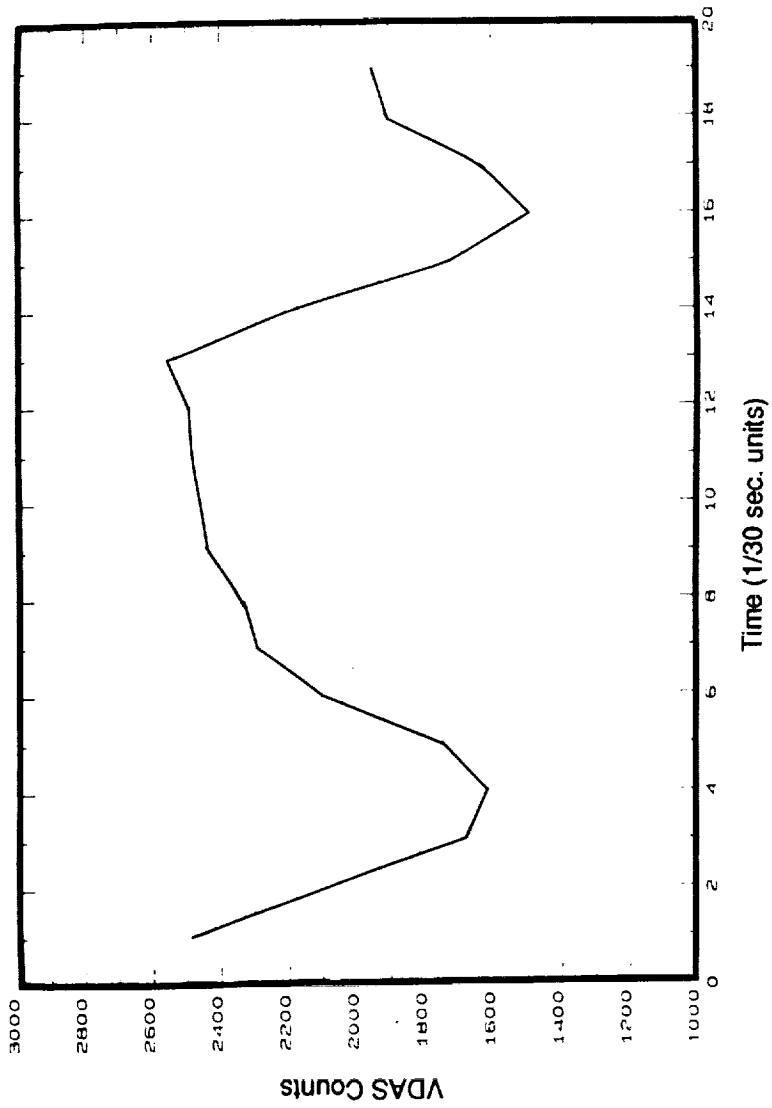


Figure 14.- Orbital debris light curve from LENZAR observations.

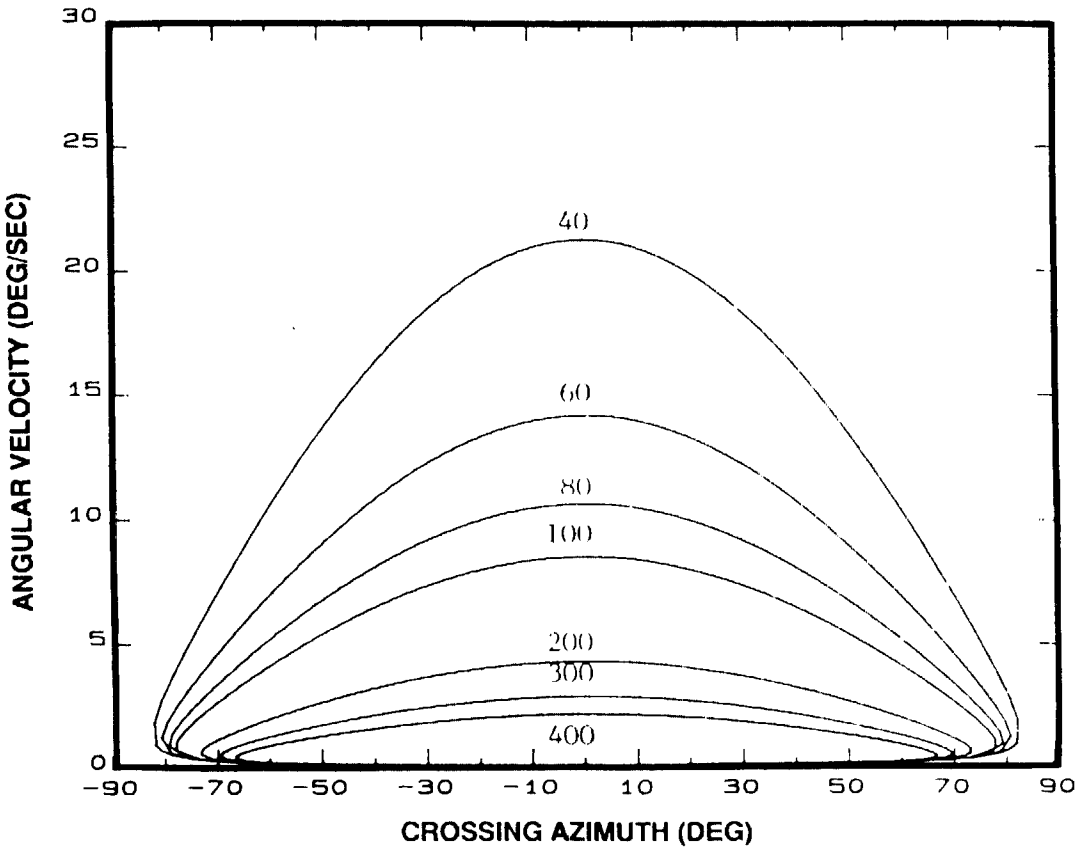


Figure 15.- IRAS constant range contours.

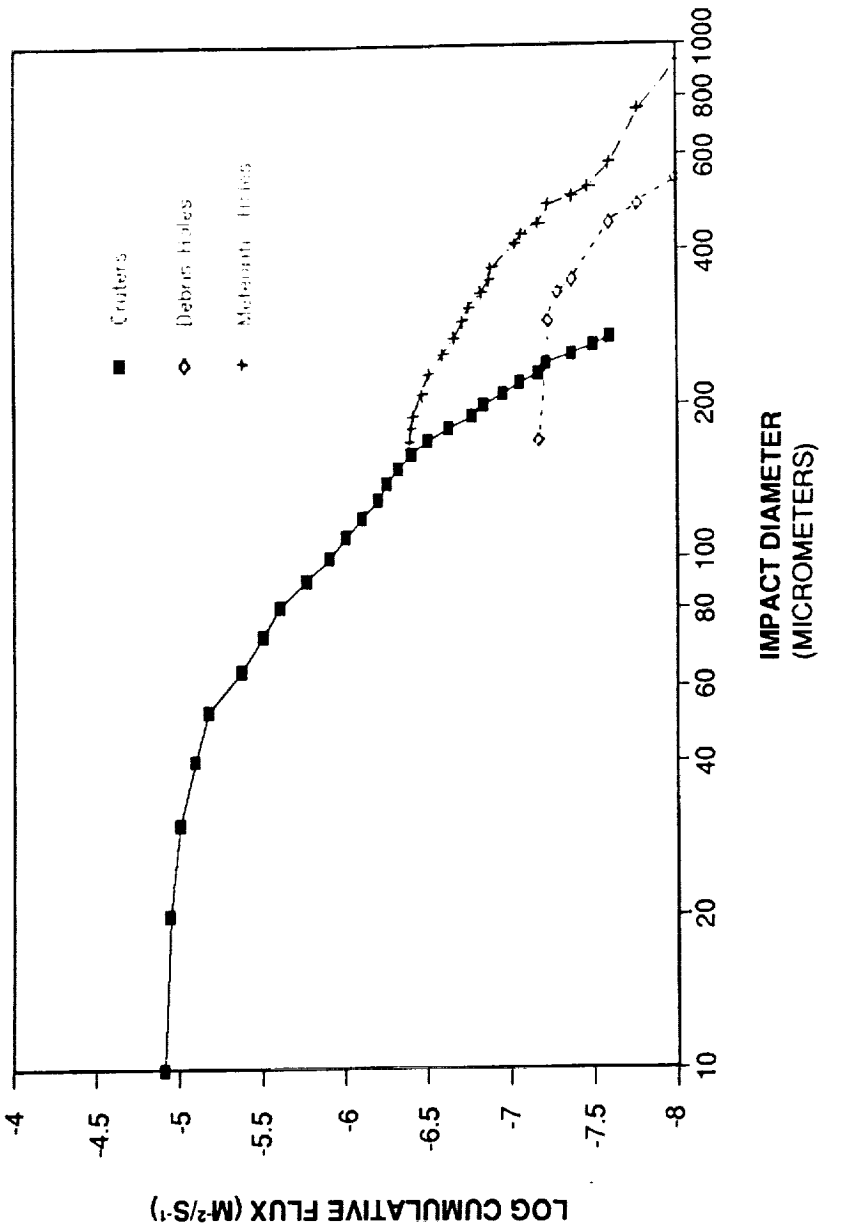


Figure 16.- Solar Maximum flux values derived from holes and craters in the thermal control louvers.

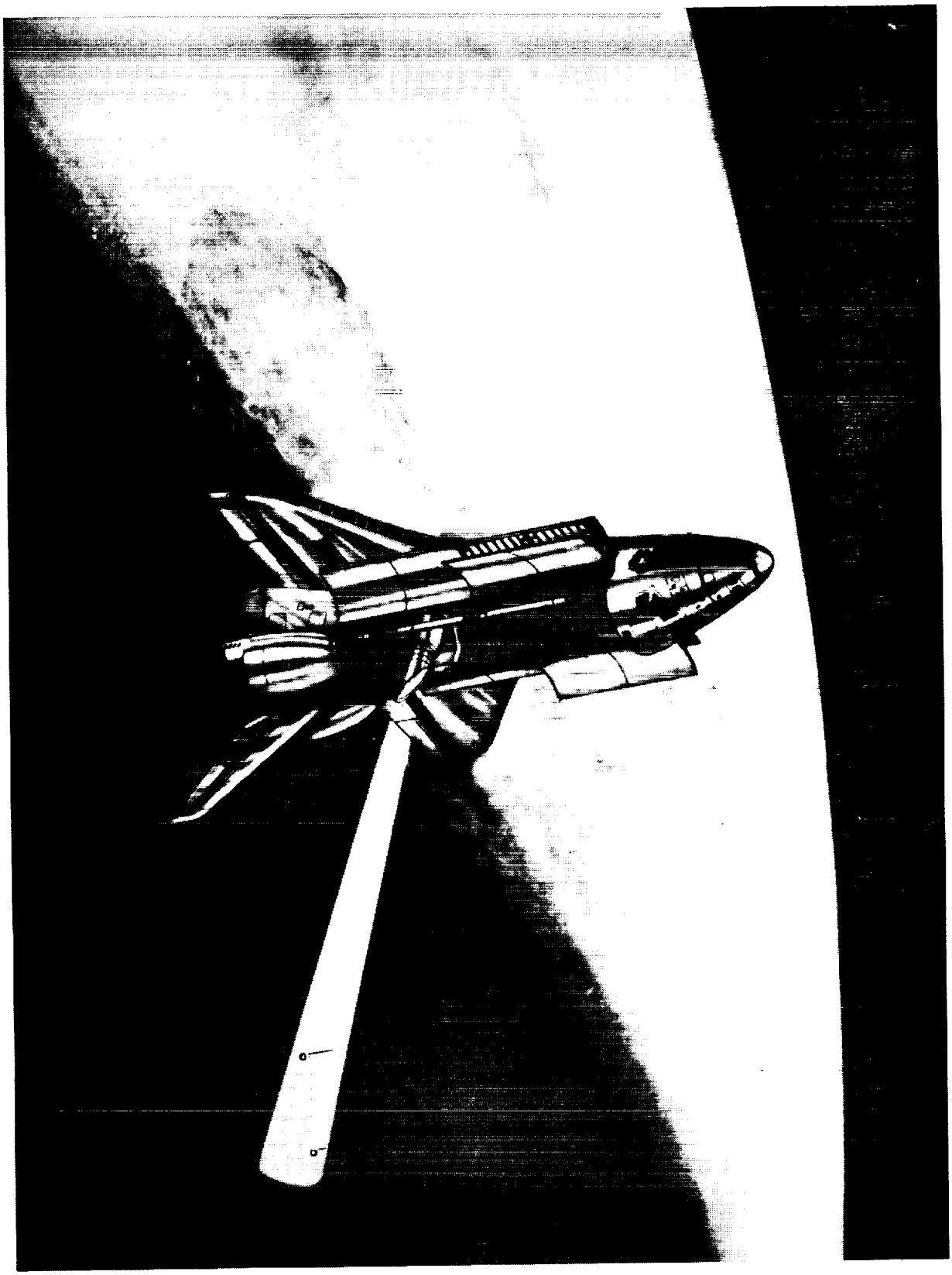

Figure 17.- Artist's concept for a space-based debris telescope.

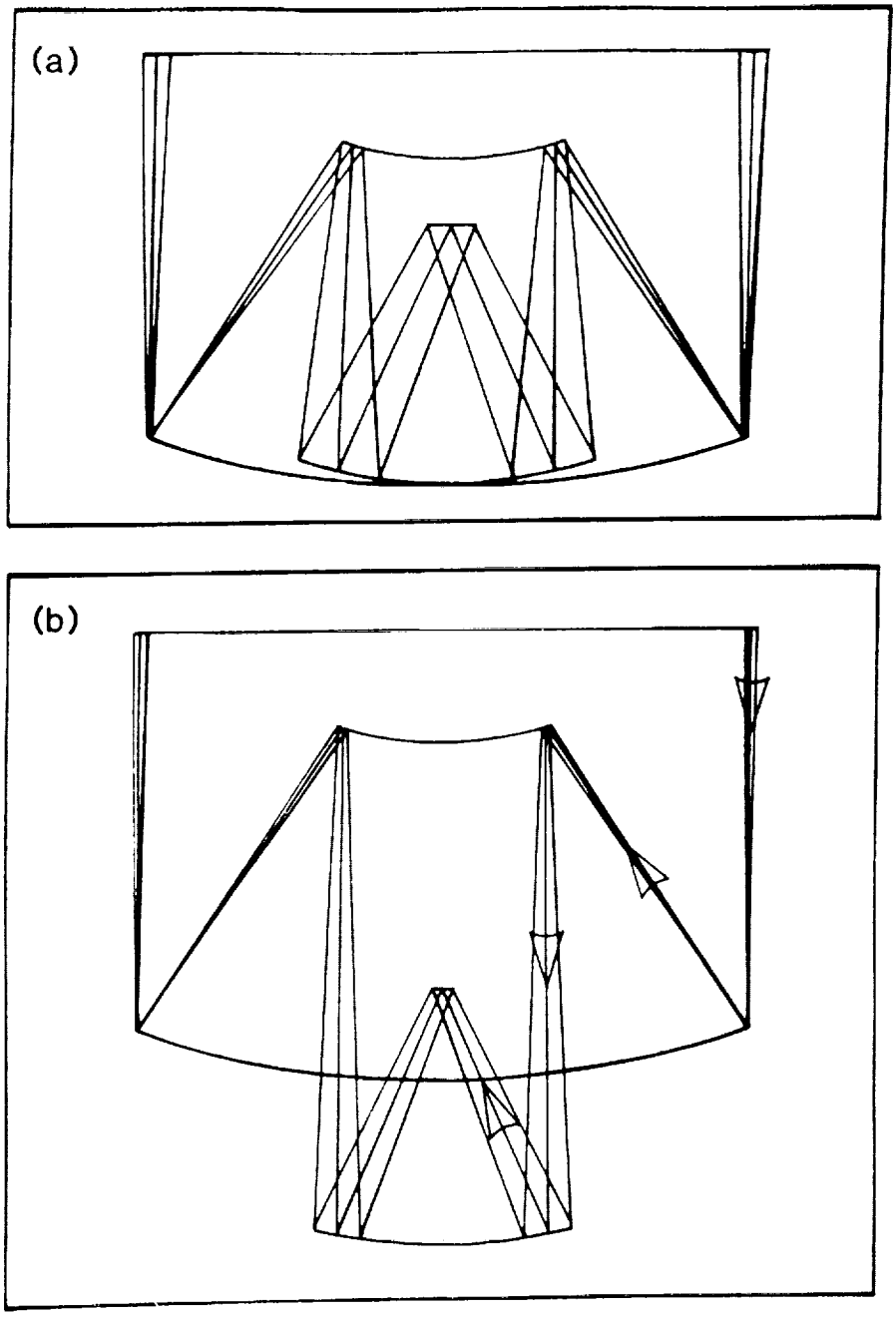


Figure 18.- Alternative all-reflecting Schmidt designs for a space-based debris telescope.


Figure 19.- The portable ground-based CCD telescope.

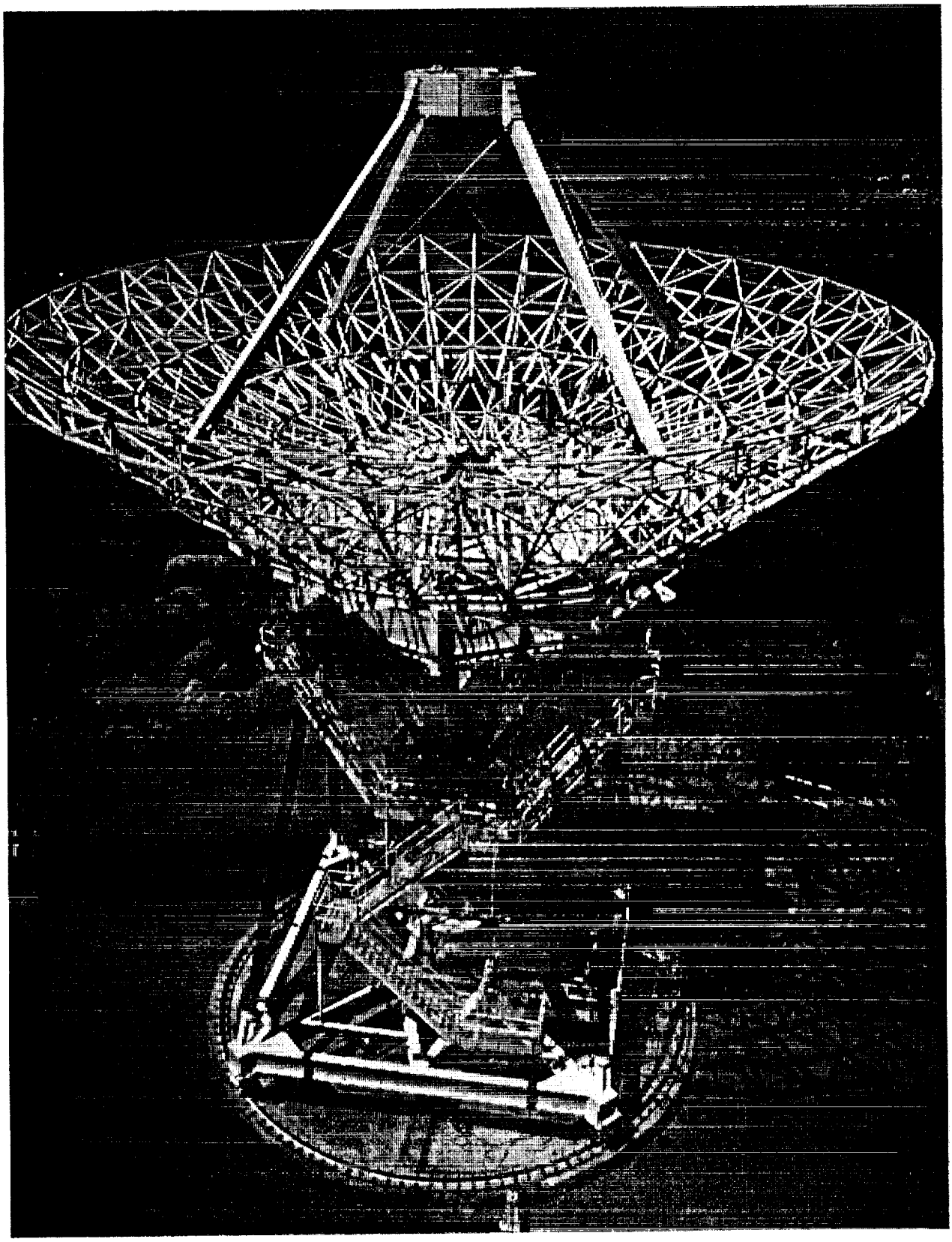

Figure 20.- A radar system, similar in size to the DECR, being used in a zenith starring mode.

# REPORT DOCUMENTATION PAGE

| 1. Report No. | 2. Government Accession No. | 3. Recipient's Catalog No. |
|---|---|---|
| NASA TM 102 155 | | |

| 4. Title and Subtitle | 5. Report Date |
|---|---|
| Orbital Debris Research at NASA Johnson Space Center, 1986-1988 | September 1989 |
| | 6. Performing Organization Code |
| 7. Author(s) | 8. Performing Organization Report No. |
| Robert C. Reynolds, Ph.D., and<br>Andrew E. Potter, Jr., Ph.D. | S-595 |
| 9. Performing Organization Name and Address | 10. Work Unit No. |
| Lyndon B. Johnson Space Center<br>Houston, Texas 77058 | |
| | 11. Contract or Grant No. |
| 12. Sponsoring Agency Name and Address | 13. Type of Report and Period Covered |
| National Aeronautics and Space Administration<br>Washington, D.C. 20546 | Technical Memorandum |
| | 14. Sponsoring Agency Code |

15. Supplementary Notes
Robert C. Reynolds, Ph.D. - Lockheed Engineering and Sciences Company
Andrew E. Potter, Jr., Ph.D. - Lyndon B. Johnson Space Center

16. Abstract
Research on orbital debris has intensified in recent years as the number of debris objects in orbit has grown. The population of small debris has now reached the level that orbital debris has become an important design factor for the Space Station. The most active center of research in this field has been the NASA Lyndon B. Johnson Space Center. Work has been done on the measurement of orbital debris, development of models of the debris population, and development of improved shielding against hypervelocity impacts. Significant advances have been made in these areas, and the purpose of this document is to summarize these results and provide references for further study.

17. Key Words (Suggested by Author(s))
Space debris
Micrometeroids
Spacecraft design

18. Distribution Statement
Unclassified - Unlimited

Subject category: 88

| 19. Security Classification (of this report) | 20. Security Classification (of this page) | 21. No. of pages | 22. Price |
|---|---|---|---|
| Unclassified | Unclassified | 60 | |

For sale by the National Technical Information Service, Springfield, VA 22161-2171